FRONTIERS OF PHYSICS

TOPICAL REVIEW
Volume 19 / Issue 1 / 13401 / 2024

Emerging memristors and applications in reservoir computing

Hao Chen, Xin-Gui Tang†, Zhihao Shen, Wen-Tao Guo, Qi-Jun Sun, Zhenhua Tang, Yan-Ping Jiang

School of Physics and Optoelectronic Engineering, Guangdong University of Technology, Guangzhou Higher Education Mega Center, Guangzhou 510006, China
Corresponding author. E-mail: †xgtang@gdut.edu.cn
Received May 17, 2023; accepted July 14, 2023

ABSTRACT

Recently, with the emergence of ChatGPT, the field of artificial intelligence has garnered widespread attention from various sectors of society. Reservoir Computing (RC) is a neuromorphic computing algorithm used to analyze time-series data. Unlike traditional artificial neural networks that require the weight values of all nodes in the trained network, RC only needs to train the readout layer. This makes the training process faster and more efficient, and it has been used in various applications, including speech recognition, image classification, and control systems. Its flexibility and efficiency make it a popular choice for processing large amounts of complex data. A recent research trend is to develop physical RC, which utilizes the nonlinear dynamic and short-term memory properties of physical systems (photonic modules, spintronic devices, memristors, etc.) to construct a fixed random neural network structure for processing input data to reduce computing time and energy. In this paper, we introduced the recent development of memristors and demonstrated the remarkable data processing capability of RC systems based on memristors. Not only do they possess excellent data processing ability comparable to digital RC systems, but they also have lower energy consumption and greater robustness. Finally, we discussed the development prospects and challenges faced by memristors-based RC systems.

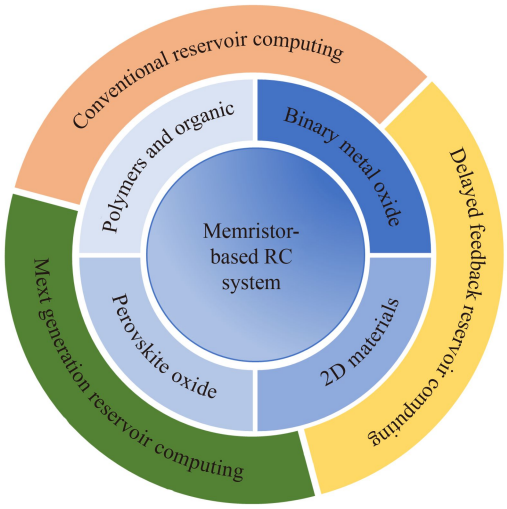

Keywords reservoir computing, memristor, resistive switching, artificial synapse, neuromorphic computing

Contents

*Special Topic: Materials, Mechanisms and Applications of Memristors (Eds.: Xiaobing Yan, Bin Gao & Qi Liu).

Higher Education Press

https://doi.org/10.1007/s11467-023-1335-x

1 Introduction

The Artificial Neural Network (ANN) is a computational model that simulates the information transmission and processing mechanisms among neurons in the human brain [1, 2]. It is composed of a large number of artificial neurons interconnected with each other, and can be used for tasks such as classification, regression, and clustering. The ANN typically consists of three layers: the input layer, the hidden layer, and the output layer. The input layer receives external inputs, the hidden layer processes the input data, and the output layer outputs the final result. Each neuron receives input from other neurons and combines these inputs weighted by activation function, and then passes the result to the next neuron. Each neuron includes an activation function and weights, where the activation function determines the output of the neuron and the weights determine the influence of the input signal on the neuron's output [3, 4]. The training process of the artificial neural network is achieved by adjusting the connection weights to make the network output as close as possible to the expected output. The Recurrent Neural Network (RNN) is an artificial neural network with short-term memory (STM) function that can be used for time series data [5, 6]. The RNN passes information from the past to the future by using the previous output as the current input. The RNN includes a hidden layer where the neurons remember the previous inputs and pass this information to the next time step. The input at each time step includes not only the current input signal but also the output result of the previous time step.

Reservoir Computing (RC) is a concept [7] that originated from RNN and has recently been successfully applied to a wide range of tasks, such as image recognition, speech recognition, time series signal processing, and chaotic dynamic system prediction. The core of RC is the use of a fixed, randomly generated neural network structure, called the "reservoir", which can nonlinearly transform the input signal and project it into a high-dimensional space, making the input signal linearly separable in low-dimensional space. By utilizing nonlinear transformation, the initial characteristics, generally presented in the temporal domain, can be projected onto the reservoir state characteristics. These characteristics can then be subjected to additional processing through a simple, trained linear neural network. Unlike traditional RNNs, RC does not require training of the reservoir pool, but achieves learning by training the output layer with linear weights. This approach enables fast training, high energy efficiency, and insensitivity to hyperparameters [8].

However, RC necessitates significant computational resources, especially when dealing with massive data. The cost of implementing RC on traditional computers is high, as it requires extensive memory and computing power. Consequently, a recent research trend is to develop Physical Reservoir Computing (PRC), which utilizes the nonlinear dynamic properties of physical systems to construct a fixed random neural network structure for processing input data. So far, RC based on photonic modules [9–11], spintronic devices [12, 13] and memristors has demonstrated highly efficient time processing. Memristor-based RC, in particular, has garnered considerable attention. The memristor is a device with memory function and nonlinear response, and its resistance depends on the history of current or voltage passing through it. This characteristic makes memristors a good choice for the reservoir in RC, generating diverse reservoir states and enhancing RC's ability to process temporal signals. For instance, the RC system based on metal oxide memristors utilizes the inherent physical state decay of themselves, allowing the system to naturally return to its initial state after receiving input signals, and achieving a type of leaky integration nonlinear dynamics [14].

In this paper, we have discussed the materials, physical mechanisms, and conductive properties of emerging memristors. Additionally, we have presented how memristors can be applied to various PRC systems optimized by diverse algorithms to process time series signals. Furthermore, we have deliberated on the prospects and challenges faced by the future development of PRC systems.

2 Investigation of storage materials of memristor

2.1 Binary metal oxide

Since the advent of solid-state memristor based on TiO_2 material by the HP team in 2008, numerous research groups have discovered memristive behavior in various oxide materials. Among them, binary metal oxide researches, such as vanadium oxide (VO_2) [15–17], zirconium oxide (ZrO_2) [18, 19], nickel oxide (NiO) [20–23], tungsten oxide (WO_x) [24–28], zinc oxide (ZnO) [29–31], hafnium oxide (HfO_2) [32–34], and tantalum oxide (Ta_2O_5) [35–38] have been widely investigated due to their simple fabrication processes and compatibilities with CMOS technology. Currently, the focus of researches is to enhance the performance of oxide-based memristors through approaches such as doping, deposition of protective layers, and electrode replacement.

The HfO_x memristor has potential for applications in nonvolatile memory and neuromorphic computing, but its continuous conduction modulation and switching linearity still require improvement. Li *et al.* [39] have fabricated a memristor with a Pt/Mg:HfO_x/TiN structure, as shown in Fig. 1(a). Unlike memristors doped with other elements previously used, the Mg-doped memristor demonstrates excellent characteristics of

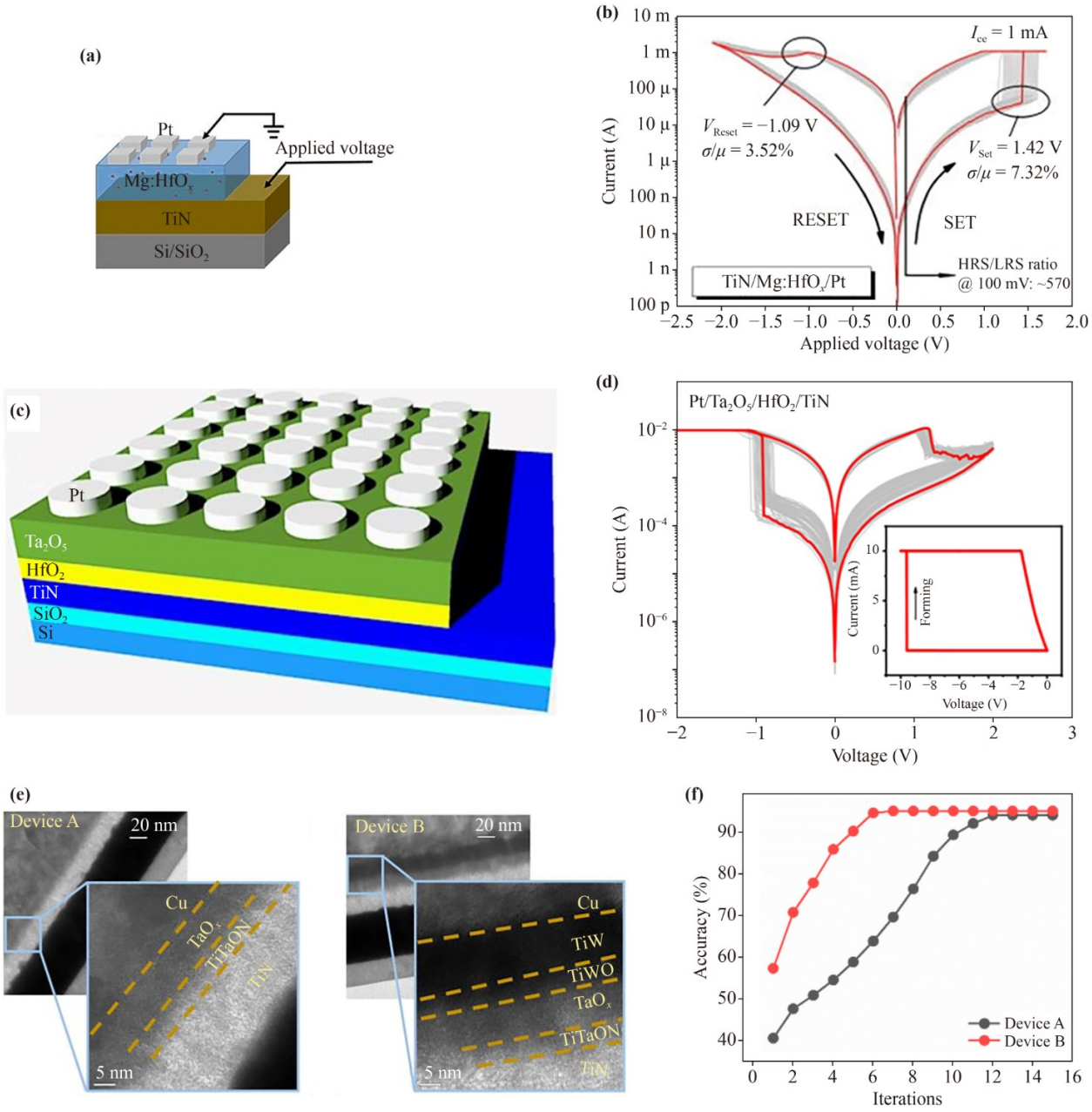

Fig. 1 **(a)** Schematic illustration of Pt/Mg:HfO$_x$/TiN structure. **(b)** The RS characteristics by changing the maximum sweep voltages. (a, b) Reproduced from Ref. [39]. **(c)** Schematic illustration of Pt/Ta$_2$O$_5$/HfO$_2$/TiN structure. **(d)** Analysis of the RS characteristics. (c, d) Reproduced from Ref. [40]. **(e)** Typical cross-sectional TEM images of device A and device B. **(f)** Neural network classification accuracy. (e, f) Reproduced from Ref. [41].

continuous conductance modulation and multilevel resistive switching (RS) under pulsed voltage, as illustrated in Fig. 1(b). The improvement in RS performance is attributed to the migration of Mg into the conductive filaments by adjusting oxygen vacancy migration and defect states, as shown by first-principles calculations and conductive mechanism analysis. It is explained that Mg doping can improve RS performance more effectively than Ca doping because of the double-ion cooperative migration of Mg^{2+} and VO^{2+}, and provides a practical way to enhance the RS performance of transition metal oxide memristors [39].

Ryu and his colleagues proposed a Pt/Ta$_2$O$_5$/HfO$_2$/TiN memristor with improving RS behavior by introducing a HfO$_2$ layer [40]. It exhibited uniform switching performance [Figs. 1(c, d)], which is due to the generation and destruction of oxygen vacancies in the HfO$_2$ layer. The device demonstrated low-power resistive switching with various synaptic plasticity, such as paired pulse facilitation (PPF), short-term potentiation (STP), long-term poten-

tiation (LTP), and spike timing-dependent plasticity (STDP), by adjusting the pulse amplitude, width, frequency and interval. Additionally, the team evaluated the pattern recognition accuracy of a 3-layer neural network composed of Ta_2O_5/HfO_2-based memristor synapses, and showed an excellent result.

To result in an improvement of RS behavior and synaptic performances, Saleem et al. inserted an oxidizable metal (TiW) diffusion barrier between the active metal electrode and the switching layer in conducting bridge $Cu/TaO_x/TiN$ memristor devices [41]. Device A, which is a sample used for reference, was created without TiW as a barrier layer. And the device made with TiW is denoted as Device B, as shown in Fig. 1(e). The TiW barrier layer serves to prevent undue diffusion of metal ions into the switching layer. Additionally, the $TiWO_x$ interfacial layer is fashioned between the barrier and the switching layer to regulate the dispersion of oxygen vacancies and facilitate the construction and dismantling of the metal ion-oxygen vacancy hybrid conducting bridge. Device A that relies on non-hybrid conducting bridges (metal ions only) performs poorly in terms of analogous performance, while a device with the barrier layer can provide 2-bit memory and 50 stable epochs. TaO_x also acts as a layer that suppresses resistance and enhances thermal conductivity, reducing overshooting current. The improved analog device featuring a high linear weight update, exhibits multilevel cell properties and steady epochs. To demonstrate the neuromorphic aspect of the devices, a simulated neural network containing 100 synapses was employed to classify 10×10 pixel images, achieving 95% accuracy with only six interactions, as illustrated in Fig. 1(f). The research provides valuable insights for optimizing synaptic performance in future neuromorphic computing applications.

2.2 2D materials

Although oxide-based memristors exhibit stable performance and mature research, traditional three-dimensional oxide memristors do not have a size advantage, making it challenging to meet the requirements of highly integrated circuits. However, with the advancement of materials, this issue has been addressed by transitioning from three-dimensional to two-dimensional structures, which is a significant research breakthrough in terms of device size reduction and achieving high integration. Currently, two-dimensional materials represented by emerging novel materials have become a popular research direction and are likely to become a focal point of future research [42, 43].

Two-dimensional materials such as graphene, with van der Waals forces connecting the layers, offer great potential for memristor applications. Whether used as a resistive switching (RS) layer or an electrode, graphene and its derivatives exhibit excellent performance. Moreover, graphene is known for its low manufacturing cost, high mechanical flexibility, and optical transparency, making it a promising material for electrodes and interface materials to enhance device performance. Chan *et al.* [44] have demonstrated outstanding performance in resistive switching, data retention, and time-dependent plasticity of graphene-based gadolinium oxide memristors, as shown in Fig. 2(a), by utilizing compact self-assembled graphene modified with hydrogen plasma as the bottom electrode, mimicking artificial synapses in neuromorphic systems.

In the conventional memristor structure, the migration of oxygen ions lacks precise control, resulting in undesirable leakage current, device-to-device and cycle-to-cycle variability, as well as device reset failures. Graphene, employed as an interface material, offers a promising solution to these issues. Zhao *et al.* [45] have utilized graphene with controlled defects to modulate the paths of cation injection and the distribution of conductive filaments, thereby achieving low operating current in memory and high driving current in selectors, as illustrated in Figs. 2(b, c). Lee *et al.* [46] have inserted graphene thin films with engineered nanoscale pores between Ta and Ta_2O_5, effectively blocking the transport of oxygen ions and redox reactions, thus enabling effective tuning of device performance by controlling the size of nanopores in grapheme, as illustrated in Figs. 2(d, e).

In addition to graphene, transition metal dichalcogenides (TMDs) have also gained significant research attention as the RS layer in memristors. TMDs, represented by MX_2 (where M represents a transition metal, such as Mo, W, Sn, Hf, and Zr, and X represents a chalcogen atom, such as S, Se, and Te), showcase remarkable aptitude in terms of electrical, optical, chemical, and mechanical properties [49]. These materials can be fashioned by enclosing a layer of transition metal atoms between two layers of chalcogen atoms via van der Waals forces. TMDs, as semiconductors, offer several advantages, such as a considerable bandgap, relatively high carrier mobility, and stability in air [50]. Naqi *et al.* [47] have achieved direct synthesis of MoS_2 thin films on patterned bottom electrodes (Pt) with high crystallinity using sputtering and chemical vapor deposition (CVD) techniques. The proposed MoS_2 memristor exhibits remarkable durability and retention, and demonstrates highly consistent memory performance in a scalable 4×4 crossbar array, as depicted in the accompanying Fig. 2(f). Functioning as synaptic devices, these memristors emulate the dynamic processes of synaptic enhancement, decay, long-term memory, and short-term memory. Furthermore, they also simulate the learning process of deep neural networks, achieving a recognition accuracy of 98.55%, differing by only 1% from software-simulated neural networks.

Yan *et al.* [48] have utilized 2H-phase WS_2 to construct a low-power memristor device with a Pd/

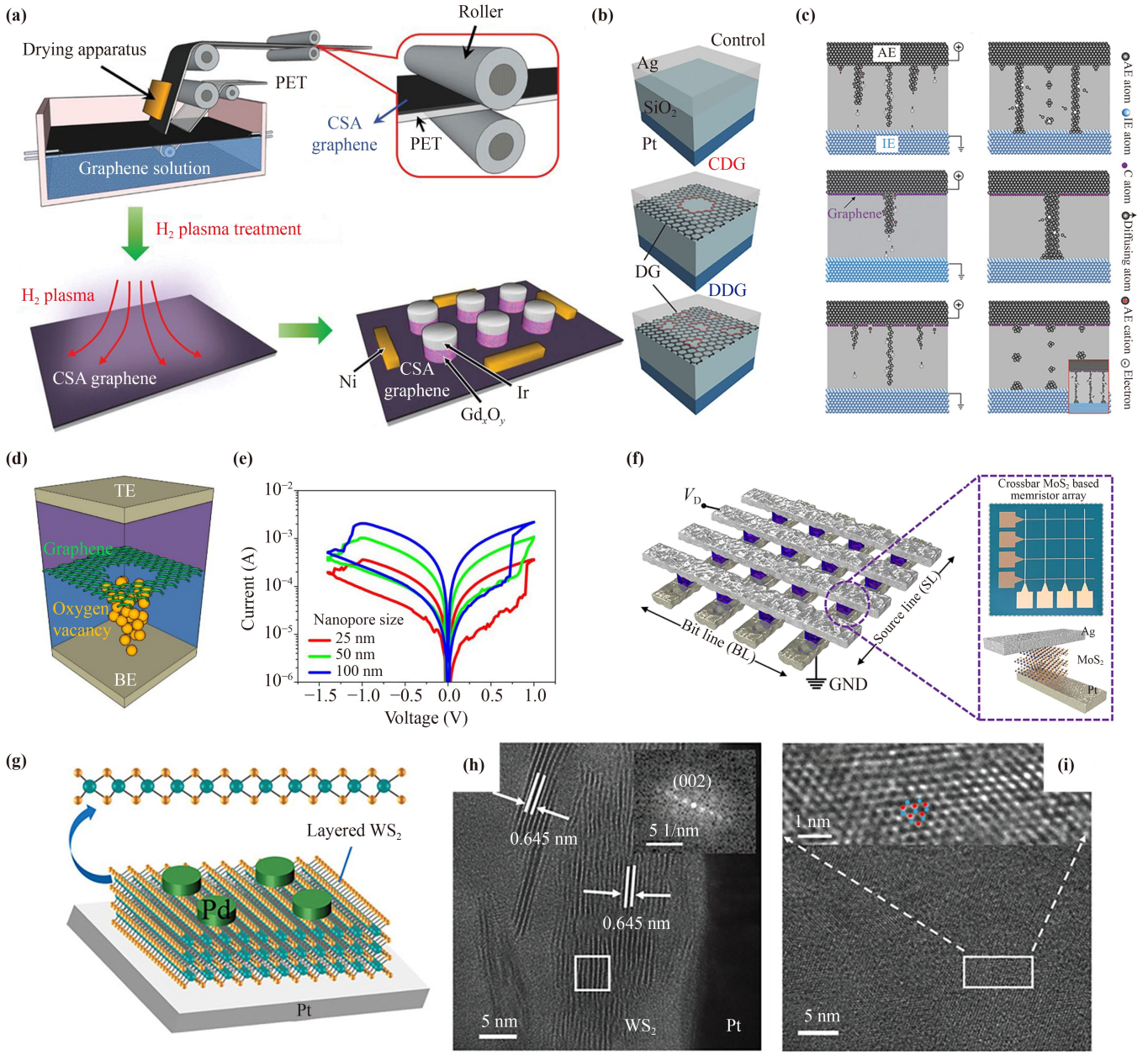

Fig. 2 **(a)** Fabrication procedures of the Gd_xO_y memristors with CSA graphene Bes [44]. **(b)** The structure of Graphene sheets with different types of defects and varying sizes/concentrations. **(c)** The process of CF modulated by defective graphene. (b, c) Reproduced from Ref. [45]. **(d)** The diagram depicts the structure of the memristor with graphene insertion. **(e)** The switching characteristics with different sized nanopores. (d, e) Reproduced from Ref. [46]. **(f)** Schematic illustration of the 4 × 4 crossbar array based on Ag/MoS2/Pt structure [47]. **(g)** Schematic illustration of the memristor with WS_2 layer [48]. **(h)** TEM and FFT images of the WS2 device. **(i)** TEM image of the different area of the WS_2 device. (h, i) Reproduced from Ref. [48].

WS_2/Pt structure, as shown in Fig. 2(g). This device exhibits a fast-switching time of only 13 ns and a low programming current of 1 μA in the ON state, with SET (RESET) energy to the femtojoule level. Transmission electron microscopy (TEM) observations reveal that the WS_2 thin film possesses a layered structure, as depicted in Figs. 2(h, i), with an increased concentration of tungsten and sulfur vacancies, which is the main reason for enhancing the resistive switching performance. This mechanism differs from the traditional metal ion conduction filament (CF) or oxygen vacancy mechanism. Furthermore, this device is capable of emulating the excitatory and inhibitory behaviors of biological neurons, as well as memory and learning under both negative and positive pulse stimulations, enabling STDP, PPF, and transitions from STP to LTP.

Hexagonal boron nitride (h-BN) is a type of two-dimensional layered insulator material, also known as white graphene. Compared to the conventional oxides, h-BN can be produced with a remarkably smooth and even surface, which has the potential to minimize fluctuations in memristor devices. In addition, h-BN has excellent chemical stability, which prevents interaction with adjacent layers, and high thermal conductivity that facilitates heat dissipation in electronic devices. In contrast to other two-dimensional conductive and semiconducting materials, h-BN can be employed to fabricate memristor devices without a transfer process. This is because it can be grown directly on a metallic substrate through CVD. Due to its insulating nature, h-BN exhibits a considerable current on/off ratio, making it a promising candidate for use in memristor devices. Shi *et al.* [51] employed CVD to fabricate electron synapses with vertical metal/h-BN/metal cell structure. The boron vacancies generated in the h-BN thin film, serving as the RS layer, induce the filling of adjacent metal ions to form conductive nanofilaments. The standby and switching power consumption can be as low as 0.1 fW and 600 pW, respectively. The switching time is less than 10 ns, and exhibits rapid (~200 μs) and stable relaxation within 500 cycles, meeting the requirements of low-power and real-time operations in artificial neural networks. This highlights the potential of h-BN in neuromorphic computing.

2.3 Perovskite oxide

Since the discovery of the electro-pulse-triggered reversible resistive switching effect in $Pr_{0.7}Ca_{0.3}MnO_3$ thin film devices in 2000, an increasing number of perovskite oxide resistive switching materials have been proposed and investigated. Subsequently, researchers have explored other perovskite oxide materials with similar resistive switching characteristics, such as $La_{1-x}Sr_xMnO_3$ [52–55] and $SrTiO_3$ [56–60]. Perovskite complex oxides are a class of compounds with the same structure as the perovskite $CaTiO_3$, which can be represented as ABO_3. Materials with perovskite structure exhibit spontaneous polarization, and the polarization direction can be rearranged along the external electric field direction under the action of an applied electric field. The materials show different current transport abilities before and after the change in polarization direction, thus exhibiting continuously variable resistance under the influence of an external electric field, presenting a memristive phenomenon. Due to the excellent properties of non-volatility, high speed, and low power consumption, perovskite materials have been widely used in electronic devices, such as non-volatile memories, resistive random-access memories, and reconfigurable logic devices. With the continuous deepening of research, the performance of perovskite resistive switching materials has been continuously improved, such as repeatable erase and write cycles, reliability, and response speed. In addition, researchers have also found that by controlling the chemical composition and microstructure of perovskite materials, or replacing the substrate, the resistive switching characteristics can be further tuned, such as controlling resistance ratio, current density, and switching voltage.

Artificial neurons play a crucial role in building neuromorphic networks, which can efficiently and in parallel compute information, akin to the human brain. However, conventional complementary metal-oxide-semiconductor (CMOS) based artificial neurons lack biological plausibility and fail to mimic the rich ion dynamics of biological neurons. To address this issue, organic-inorganic halide perovskites (OHPs) have emerged as a promising candidate for mimicking ion dynamics in biological neurons, owing to their intrinsic ion migration [63, 64]. A diffusive memristor based on $CH_3NH_3PbI_3$ ($MAPbI_3$) has been fabricated [Fig. 3(a)], which exhibits exceptional amplitude-frequency characteristics and substantially linear modulation of conductivity, capable of achieving over 1000 states [61]. This memristor has been employed in the creation of a bio-inspired neuron, named the leaky integrate-and-fire (LIF) neuron, which adeptly replicates the leakage, spatiotemporal integration, and firing functionalities of natural neurons. Furthermore, through the interconnection of LIF neurons using a 2×2 non-volatile Al_2O_3-based synaptic array, a simple spiking neural network (SNN) has been effectively constructed at the hardware level. The SNN exhibits remarkable discerning sensitivity to particular input sequences, thereby demonstrating the potential for future applications in neuromorphic computing that incorporate innovative ionotropic devices.

Presently, the majority of perovskite materials are cultivated on substrates composed of single crystals [65]. Regrettably, the incompatibility of complex oxides with silicon technology used in complementary metal oxide semiconductors poses a major obstacle in the integration of the two. $BiFeO_3$ is the only material that exhibits multiferroic properties at room temperature, making it a promising candidate for applications [66]. However, it has certain drawbacks such as large coercivity field voltages and high leakage currents, which can be improved through doping. As such, Wang and his colleagues [62] have constructed a memory resistor with a sophisticated structure composed of $Pd/Li_{0.09}Bi_{0.91}FeO_3/La_{0.67}Sr_{0.33}MnO_3/SrTiO_3/P^{+-}Si$. The $SrTiO_3$ layer is grown on Si as a buffer layer, and the $BiFeO_3$ layer doped with Li serves as the functional layer [62], as shown in Figs. 3(c–h). This device exhibits remarkable stability, reproducibility, and continuous tunability. Moreover, by modulating the electrical conductivity through the application of different parameter pulses, it emulates the synaptic function of neurobiology. Importantly, multiple devices can be interconnected into prac-

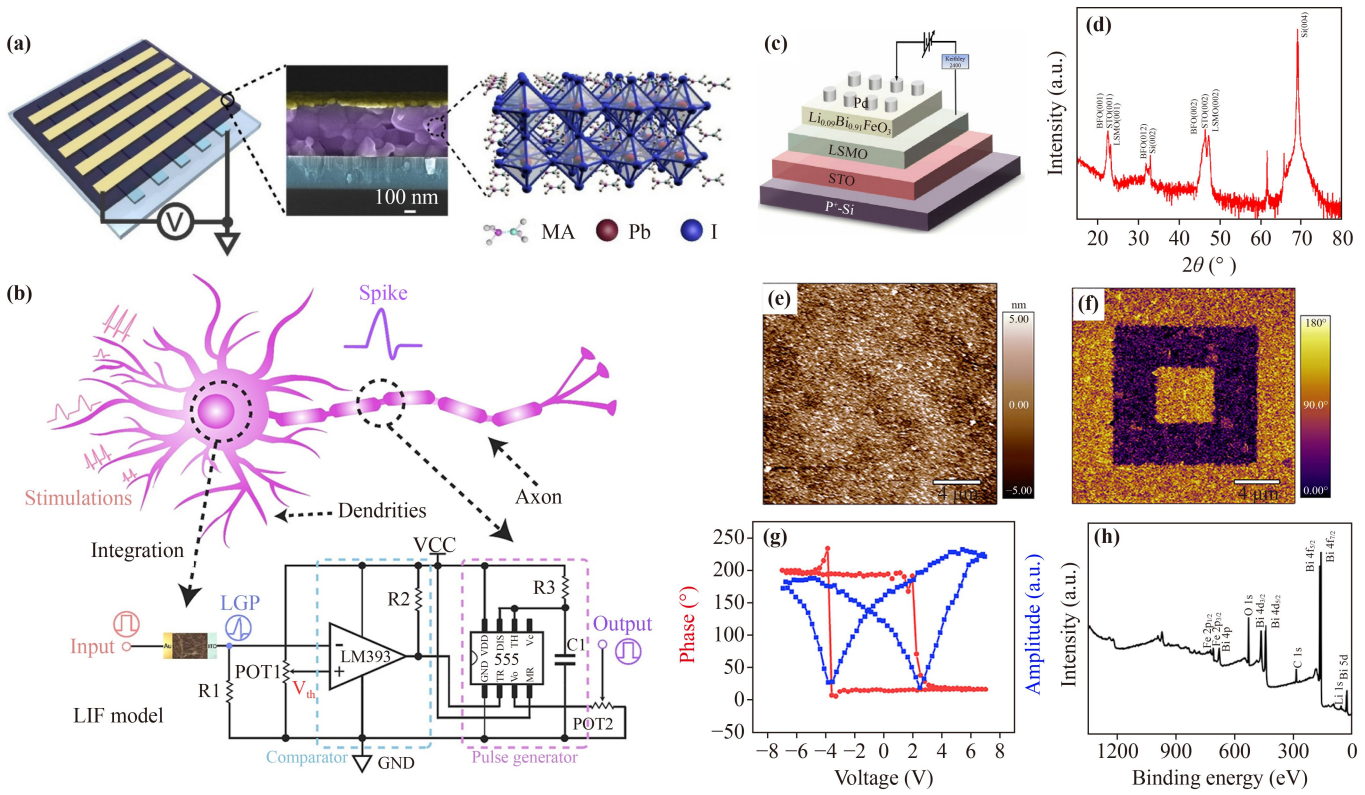

Fig. 3 **(a)** Schematic diagram of the Au/$MAPbI_3$/ITO memristor, cross-sectional SEM image of the memristor and molecular structure. **(b)** Schematic illustration of a biological neuron and its experimental circuit. (a, b) Reproduced from Ref. [61]. **(c)** The structure of the Pd/LBFO/LSMO/STO/Si device. **(d)** XRD patterns. **(e)** AFM morphology diagram. **(f)** PFM phase diagram. **(g)** PFM hysteresis loop. **(h)** XPS full spectrum. (c–h) Reproduced from Ref. [62].

tical circuits, enabling information storage and addressing the issue of resistance drift. The output current linearly increases with the number of conducting devices, and information encoding/decoding is achieved through circuitry, offering the possibility of neuromorphic computing and information processing.

In addition, Su *et al.* [67] developed a memristor with the structure of Au/$SrFeO_x$(SFO)/$SrRuO_3$ (SRO) that exhibits repeatable polarity reversal behavior. The application of an appropriate reverse bias voltage can reverse the direction of the set and reset voltage, and the cycling stability and retention performance of the SFO device remain unaffected by the polarity of operation. The cross-sectional transmission electron microscope (TEM) image illustrates a distinct interface between each layer in the synthesized Au/BM-SFO/SRO device, and the corresponding energy dispersive spectroscopy (EDS) images demonstrate the even distribution of elements in each layer, as depicted in Figs. 4(a–g). X-ray photoelectron spectroscopy (XPS) analysis indicates that oxygen ions migrate during the polarity reversal process. First-principles calculation of energy band structure suggests that an insufficient amount of oxygen injection into the BM-SFO barrier layer can lead to a reduction in the band gap of BM-SFO, thereby forming a PV-SFO/BM-SFO_+ interface with a lower Schottky barrier height, facilitating Schottky emission and conduction, as illustrated in Figs. 4(h–q). The SFO device displays a remarkable accuracy of 98.81% in handwritten digit recognition and faster convergence speed on negative set status due to better synaptic weight update linearity. In summary, the alternated polarity reversal features of the SFO memristor offer a new reference for resistive memory and synaptic memristors.

2.4 Polymers and organic materials

Organic materials used in memristors are capable of reversible switching between high and low resistance states under the influence of voltage, with the advantages of low cost, simple structure, and facile fabrication processes, as well as high flexibility. They find wide applications in wearable, flexible, and implantable devices. There are diverse types of organic materials for memristors, including polymer memristors, small molecule organic memristors, and organic-inorganic hybrid memristors. Among them, polymer memristors, such as polyaniline (PANI) [68–70] and poly(3,4-ethylenedioxythiophene) (PEDOT) [71–73], are the most common type of organic memristors. They undergo redox reactions under external electric fields, leading to changes in resistivity. Small molecule organic memristors

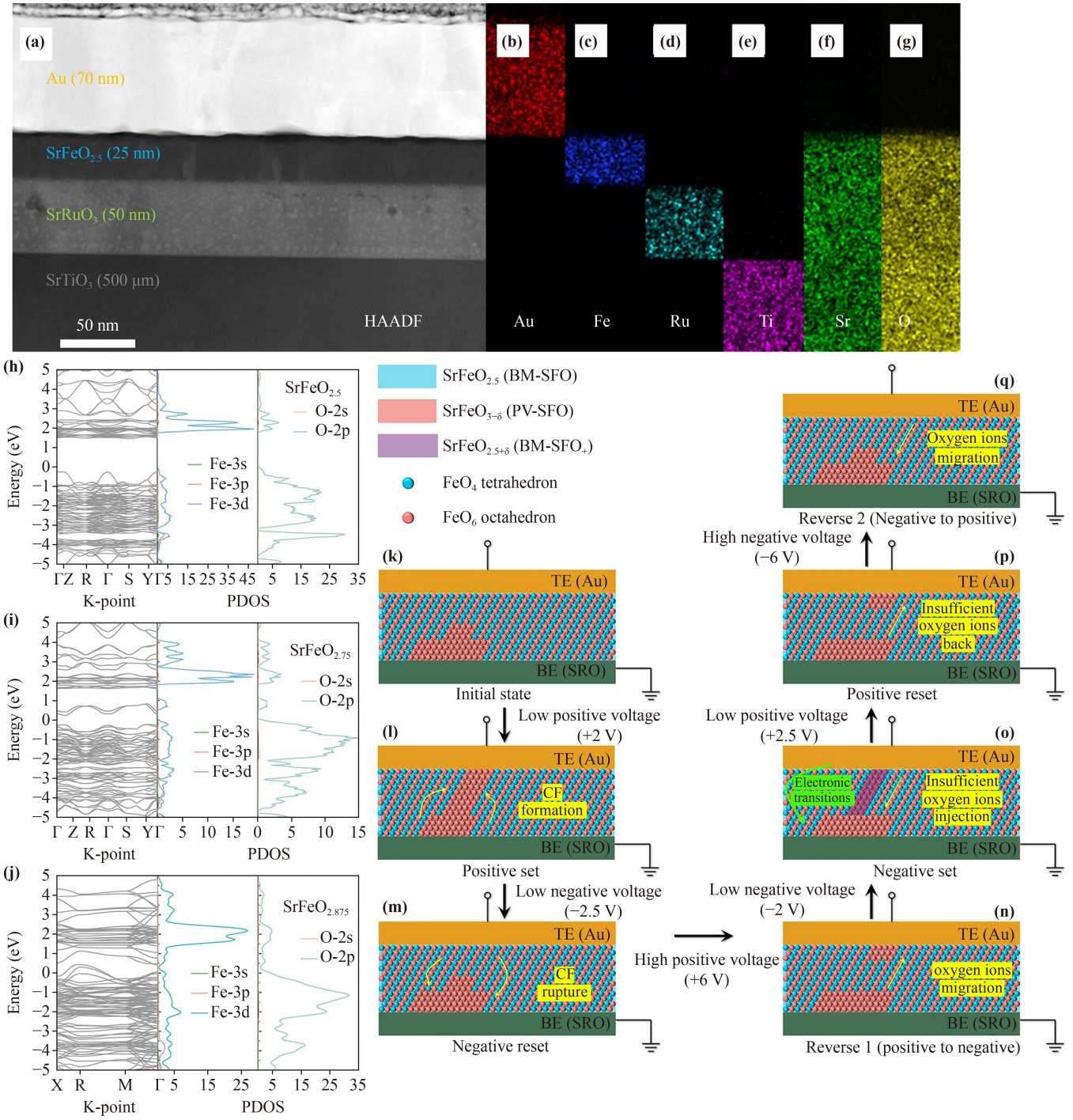

Fig. 4 **(a)** Cross-sectional HADDF TEM image of the Au/BM-SFO/SRO device. **(b–g)** The corresponding EDS mapping image of elements. First-principles calculation for band structures. **(h–j)** Band structure and PDOS plots of $SrFeO_x$. **(k–q)** Schematic RS process in the SFO memristor. (a–q) Reproduced from Ref. [67].

(AIDCN [74–76], Alq_3, etc.) also operate based on similar principles, with their molecular structures typically containing one or more controllable redox centers. Biomaterial-based memristors utilize organic biomaterials, such as DNA and proteins, as their active layer. They operate based on the reversible formation and rupture of conductive filaments between the two electrodes, and have shown potential for bio-inspired computing and memory applications.

Taking inspiration from the unique poly-ionic properties of ammonium polyphosphate (APP), Zhao *et al.* [77] have developed a new flexible and stable Au/APP/ITO memristor, as shown in Figs. 5(a–d), capable of exhibiting synaptic behavior in response to voltage pulses of 0.1 V

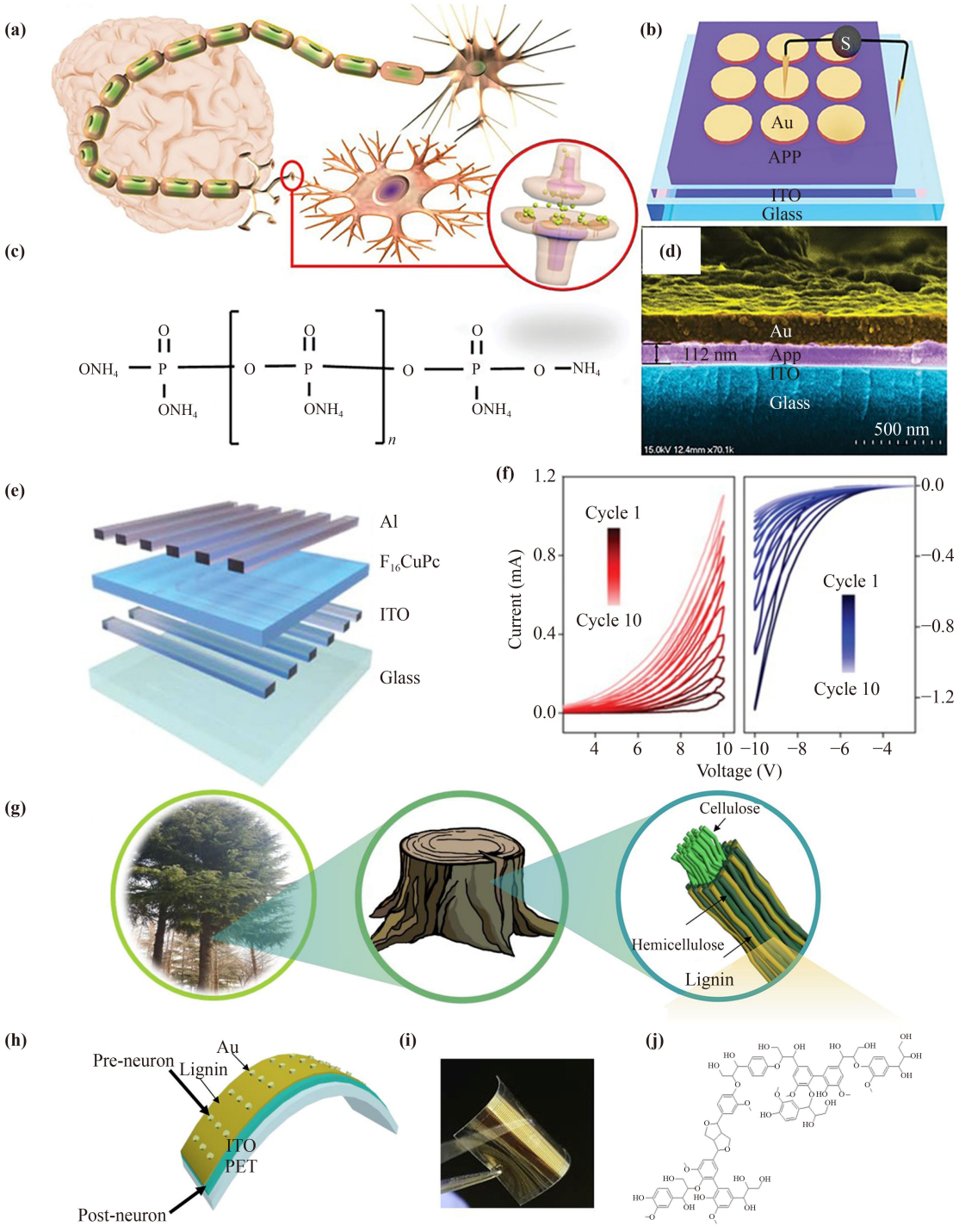

Fig. 5 **(a)** Schematics illustration of a synapse how to work. **(b)** Device structure based on APP. **(c)** Chemical structure of APP. **(d)** The cross-section of APP-based device. (a–d) Reproduced from Ref. [77]. **(e)** Schematics diagram of the ITO/F_{16}CuPc/Al device. **(f)** The switching characteristics of the F_{16}CuPc-based device with multiple sweep voltage. (e, f) Reproduced from Ref. [78]. **(g)** Lignin is widely found in plants. **(h)** Schematics diagram of Au/lignin/ITO/PET device. **(i)** Schematics diagram of the flexible memristor. **(j)** Schematics diagram of chemical structure of lignin. (g–j) Reproduced from Ref. [79].

amplitude and 20 ns width. The device outperforms several other established memristors, exhibiting repeatable synaptic behavior for up to 10^4 pulse cycles. Moreover, the memristor remains functional even when bent at 360°, and is capable of retaining its synaptic performance even after being subjected to 60 seconds of fire exposure and 5.6 kGy of ionic irradiation. In addition, APP is found to be transparent, nontoxic, and biodegradable, distinguishing it from other organic and inorganic materials used in previous memristor studies [77].

Li *et al.* [78] presented a new type of organic memristor based on a small molecule material $F_{16}CuPc$, as shown in Fig. 5(e), that is highly resistant to high humidity conditions. The devices demonstrated remarkable stability in moisture, maintaining their switching behavior even after a year of exposure to air at 60% relative humidity and after being submerged in water for 96 hours. The researchers identified a proton conduction mechanism as the cause of the resistive switching effect. The devices also showed continuously adjustable conductance, as illustrated in Fig. 5(f), allowing them to emulate the functions of biological synapses. These findings provide a promising pathway, a neuromorphic computing system, tolerant to high humidity, has been developed utilizing artificial synapse devices that demonstrate exceptional resistance to humidity.

Lignin, which is an organic component of wood [Fig. 5(g)], is a complex and random 3D network polymer consisting of intricate aromatic structures [Fig. 5(j)]. It is a plentiful natural substance on the planet and is a byproduct of the pulp and paper industry. Compared to other polymers, lignin has a high carbon content, and when subjected to heat, it can be converted into amorphous or graphitic structures, which can alter its electrical conductivity. Park *et al.* [79] have ingeniously designed a memristor with a structure of Au/Lignin/ITO/PET, as shown in Fig. 5(h). The equipment displayed a progressive modification in its conductivity when successive voltage pulses were administered, and it also remained functional without significant fluctuations when subjected to bending [Fig. 5(i)]. Moreover, the synthetic synaptic device constructed from lignin successfully imitated fundamental synaptic properties such as potentiation/depression, excitatory post-synaptic current (EPSC), spike-rate-dependent plasticity (SRDP), and the transition from STP to LTP. Due to its nontoxic, ecologically benign and biodegradable properties, lignin exhibits great potential as a crucial component for flexible electronic devices and artificial synapses [79].

3 Memristor-based reservoir computing systems

3.1 Conventional reservoir computing

Recurrent neural network (RNN) is a species of ANN that is capable of processing sequential data, for example, time series or natural language [80]. It comprises feedback connections that enable the utilization of output from previous time steps as input for the current time step, so that the network has the ability to process time series data. Therefore, RNN is better suited for simulating the dynamics of the brain system. Currently, RNN has been widely applied in tasks such as speech recognition and natural language processing. However, due to the issues of gradient vanishing and explosion [81], RNN requires a multitude of hyperparameters and has a complex training process. To address these issues, Jaeger suggested using an echo state network (ESN) [8], while Maass *et al.* [82] proposed a liquid state machine (LSM). ESN and LSM are essentially the same and are commonly referred to as RC. It is worth noting that, compared to standard RNNs, the reservoir itself does not require to be trained, RC only requires training of the output layer weights and does not need backpropagation algorithm, effectively avoiding the issue of gradient vanishing. Therefore, it can significantly reduce the complexity and duration of training.

The inherent characteristics of memristors, such as their STM and nonlinear behavior, make them highly suitable for incorporation into physical RC systems. In RC systems, several key characteristics of the reservoir significantly influence the system's performance, among which the richness of the reservoir state is one of the most critical parameters. The conductance of the memristor is often regarded as a reservoir state, and different training pulses modulate the conduction of the device, making it applicable for RC systems used in neural activity analysis. When a series of training pulses are applied with short intervals, the device exhibits an increased current, while long intervals between adjacent pulses result in a decay of the current toward a resting state. Therefore, temporal pulses with different intervals lead to distinct final states of the device, corresponding to different reservoir states. In this case, the post-stimulus state of each memristor represents the characteristic value of the given sequence of pulses for reservoir computation. By collecting the device states, pattern recognition can be achieved by simply reading out the functionality.

Zhang *et al.* [83] have established a RC system based on P3HT@TDA-PW memristors. A total of 100 memristors were utilized within the reservoir framework, and a single-layer perceptron with 100×3 neurons was employed for classification. The current readout from the memristors in the reservoir was used as input to the single-layer perceptron with three output neurons representing the emotional states of interest, namely fun, sad, and silence. The output of the system was calculated based on the dot product of the input and the weights of each output neuron using a supervised logistic regression algorithm, with weight adjustments made during training to minimize output errors, as shown in Figs. 6(a, b). After 2100 training iterations, the P3HT@TDA-PW memristor RC system was able to correctly identify the three original emotional symbols in the entire training dataset. Further exploration of the reservoir's temporal information processing capability was conducted using other samples outside of the original training dataset. Identification accuracy curve and false-color confusion matrix were plotted, respectively, to monitor the algorithm's classification performance [Figs. 6(d, e)]. To

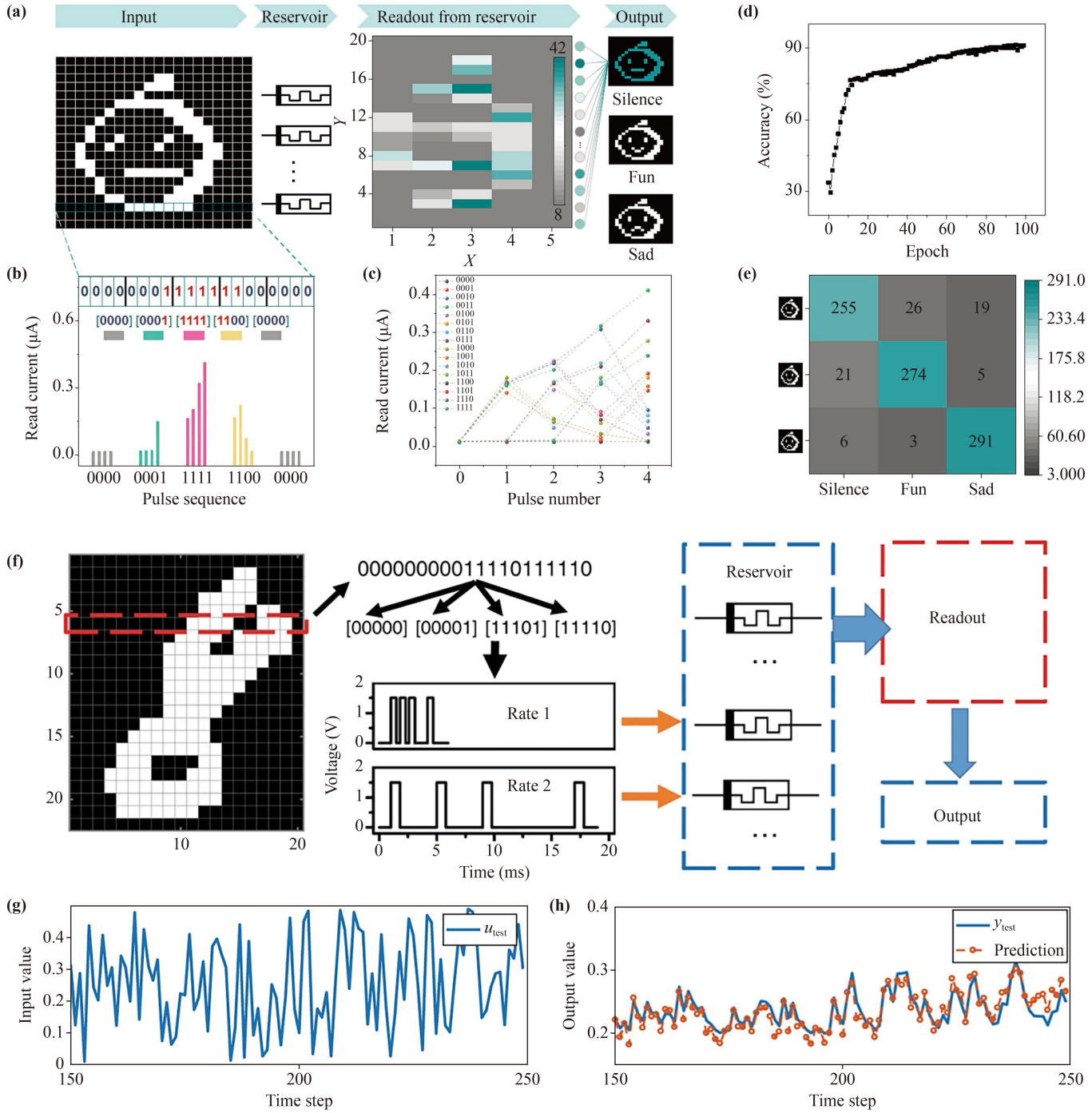

Fig. 6 **(a)** The process of emoticon recognition. **(b)** The pixel image is converted into pulses of current of different amplitudes. **(c)** Current response to 16 pulse streams and 14 states can be separated efficiently. **(d)** Relation between classification accuracy and training epochs. **(e)** False color confusion matrix. (a–e) Reproduced from Ref. [83]. **(f)** The process of handwritten digit recognition. **(g)** Random input signals u test(k) are used to solve a second-order nonlinear dynamic problem. **(h)** The forecasting results from the memristor-based RC system. (f–h) Reproduced from Ref. [84].

further evaluate the image recognition capability of the RC system, a manual digit categorization undertaking was executed employing samples from the Modified National Institute of Standards and Technology (MNIST) dataset, with an accuracy of 89.4% after trained.

Lu and his group [84] have harnessed the internal short-term ion dynamics of memory resistor devices to propose an RC system based on dynamic WO_x memristors. Through experimental verification, they have demonstrated that even a small reservoir which is composed of 88 memristor devices can be employed for handwritten digit recognition [Fig. 6(f)], as trained and

tested with the MNIST dataset, achieving an impressive recognition accuracy of 88.1%. The performance of this system rivals that of a single-layer neural network with 7850 free parameters. Similarly-sized networks have also been utilized for solving second-order nonlinear dynamic problems, successfully predicting expected dynamic outputs [Figs. 6(g, h)] without prior knowledge of the transfer function.

Milano *et al.* [85] have documented the phenomenon of material reservoir computing within a fully memristive architecture based on self-organized nanowire networks. By virtue of the functional synaptic connections endowed with nonlinear dynamical characteristics and fading memory properties, the designless nanowire complex network assumes the role of a physical reservoir spanning the entire network, offering a bottom-up approach to constructing a PRC system. Matsukatova and colleagues [86] have proposed a fully organic RC system comprised of a PANI-based organic memristive devices (OMDs) reservoir and a PPX-based OMDs spiking readout layer. Leveraging the rich dynamics of voltage-dependent switching times in PANI-based OMDs, the reservoir is capable of extracting key features from a 3-bit input. Furthermore, the spiking readout layer exhibits exceptional robustness to variations in memristive characteristics, demonstrating only minimal accuracy degradation in the presence of significant variability. Prudnikov *et al.* [87] have presented a model of an RC system featuring PANI-based organic memristors as the reservoir. This system exhibits significant robustness to variations in the internal states of the reservoir. Even if the standard deviation of the reservoir states increases by threefold, the classification accuracy of handwritten digits in the MNIST dataset does not experience a substantial decline. Koroleva and colleagues [88] have presented an introduction to self-aligned CMOS-compatible W/WO_x/HfO2/Ru cell in a 3D vertical memristive structure for RC systems. By employing the vertical structure with an array stacking, the synaptic density of the devices can be further enhanced.

3.2 Delayed feedback reservoir computing

As the performance of an RC system heavily relies on the dimensionality of the reservoir space, enhancing the RC system's performance by increasing the number of nodes in the reservoir becomes crucial [14]. Appeltant *et al.* [89] employed a reservoir layer that maps temporal information to spatial domain using a nonlinear node for transformations and a delayed-feedback line. Along the delayed line, virtual nodes can be defined to mimic the presence of numerous nodes in the convention network approach. By leveraging the dynamic characteristics of the system, particularly the different time scales, virtual interconnectivity can be created without the need for many physical connections between all virtual nodes. The system's inertia introduces coupling between adjacent virtual nodes, while the delayed feedback line accounts for the strong self-coupling of each node with its previous version. When tapping the delayed line at the position of virtual nodes, the corresponding vector represents the reservoir state [90]. The delayed coupling in the system involves a continuous time interval $[t–\tau, t]$, where τ is the delay time, which mathematically renders the state space infinite-dimensional. Although the dynamics of the time-delay system are still finite-dimensional in practice, it exhibits high dimensionality and short-term memory [89].

The training process of single-node delayed systems aligns with the traditional network approaches of RC. However, the fact that the input to the virtual nodes requires to be introduced through a nonlinear node introduces preprocessing of the input (time-multiplexing), known as masking. Setting the masking has two purposes: serializing the input and maximizing the effective utilization of the system's dimensionality. In the conventional network approach, all nodes in the reservoir layer can be directly accessed via direct connections from the input layer. In the delayed feedback approach, the input signal undergoes a nonlinear transformation at the nonlinear node and then propagates to the virtual nodes through the delayed line. Time-multiplexing is used to provide the input signal with appropriate scaling to the corresponding virtual nodes. Thus, the input scaling also needs to be imprinted on the input before injection. The result is a piecewise constant input sequence with constant intervals corresponding to the gaps between virtual nodes on the delayed line [90]. Building the reservoir using a single physical nonlinear node influenced by delayed feedback enriches the dimensionality of the reservoir space compared to traditional reservoir approaches. The use of RC methods based on linear time-delay systems with a single physical node influenced by delayed feedback is appealing for hardware implementations using emerging devices.

Huaqiang Wu and colleagues [91] have ingeniously devised a novel RC system, predicated upon dynamic memristors, that artfully employs a controllable mask process to generate a diverse spectrum of reservoir states, thereby augmenting the overall system performance, as shown in Fig. 7(a). The mask process confers the ability to finely tune the richness of reservoir states and feedback strength, two key factors that profoundly influence the performance of the RC system. Notably, the memristor's response to input signal is directly harnessed as the reservoir state, deftly leveraging the device's inherent nonlinearity and obviating the need for supplementary read operations. Furthermore, the nonlinear region of the system can be deftly modulated by manipulating the input signal range. Through meticulous calibration of these system parameters, the implemented RC system shows efficient processing of temporal signals. The efficacy

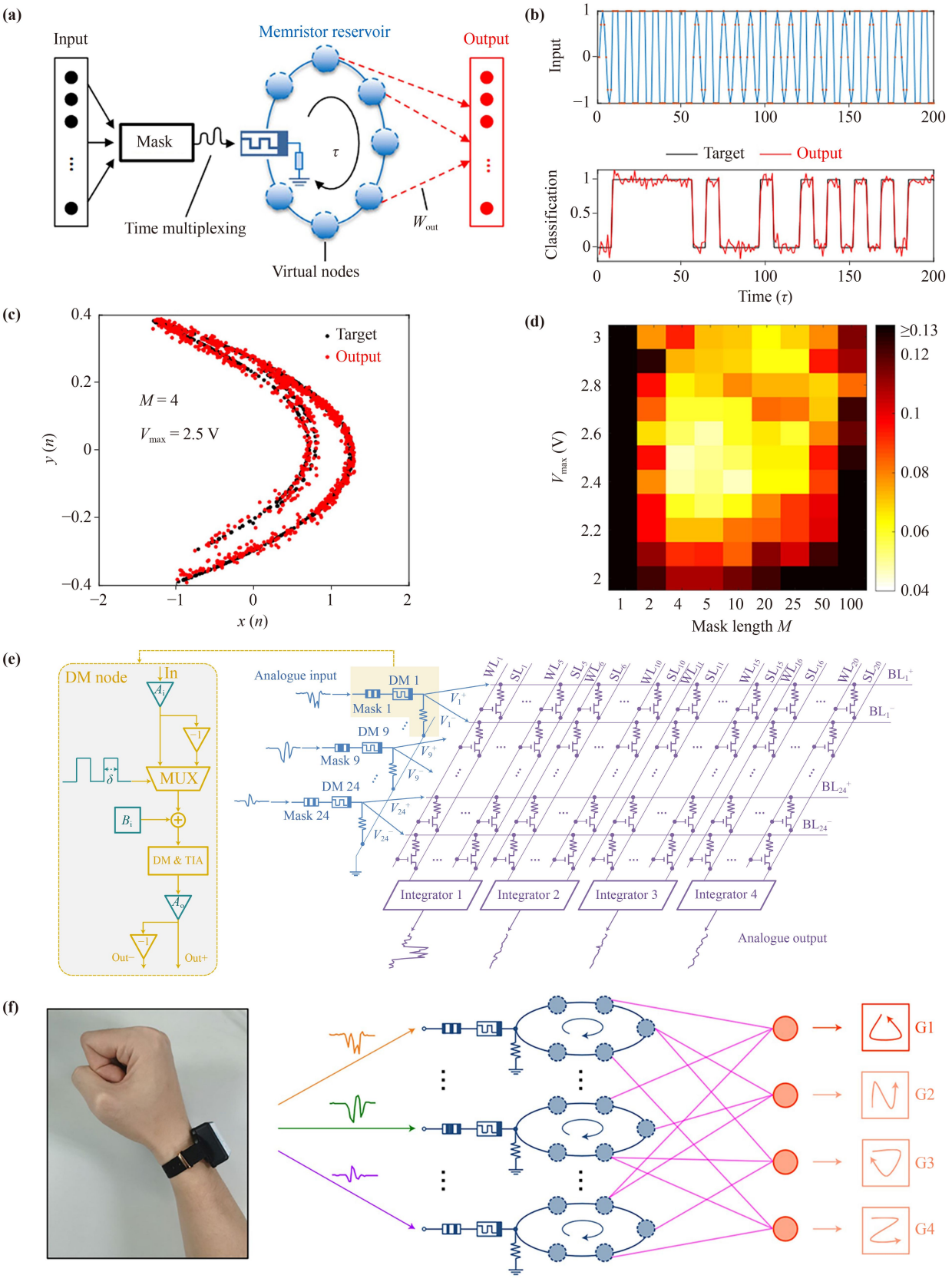

Fig. 7 **(a)** Schematics illustration of dynamic memristor-based RC system with virtual nodes. **(b)** The input and classification outcome of sinusoidal and square waveforms. **(c)** The result of Hénon map prediction. **(d)** The prediction error varies with the two test parameters M and V_{max}. (a–d) Reproduced from Ref. [91]. **(e)** Schematics diagram of the DM-RC hardware system. **(f)** Memristor-based RC system used to realize dynamic gesture recognition task. (e, f) Reproduced from Ref. [92].

of the RC system is rigorously evaluated across diverse temporal classification tasks, including waveform classification and spoken-digit recognition [Fig. 7(b)], where it attains commendably low normalized root mean square error (NRMSE) of a mere 0.14, and word error rate of 0.4%, respectively. Additionally, a time-series prediction task of the Hénon map is accomplished [Figs. 7(c, d)], yielding a remarkably low prediction error (NRMSE) of 0.046, which is merely half the value obtained by a standard echo state network (ESN). In subsequent work, the team has devised a fully analog RC system founded upon virtual nodes [Fig. 7(e)], utilized for arrhythmia heartbeat detection and dynamic gesture recognition [Fig. 7(f)], fabricated employing a Ti/TiO_x/Pd stack for the reservoir and a TiN/TaO_x/$HfAlO_y$/TiN stack for the readout array [92]. This approach permits direct signal transmission and processing without any conversion or buffering. By adjusting the hyperparameters, the dynamic memristor-based RC system capably undertakes various spatiotemporal signal processing tasks in real-time with exceptionally low power consumption, which is at least three orders of magnitude lower in comparison to digital-signal-based approaches. If this dynamic memristor-based RC system can be employed as a fundamental unit for constructing more intricate systems, it would yield a more abundant state of storage and greater storage capacity, thereby further enhancing the performance of the system, which portends immense potential in the field of edge computing in the future.

Recently, an intriguing idea has been proposed and confirmed, which combines memristor-based RC systems with neural probes for on-site, real-time processing of neural signals [93]. Specifically, the research group has designed a perovskite halide-based memristor with extremely low switching voltage of less than 100 mV and a current ranging from 1–100 nA, as well as short-term memory effects, to serve as the reservoir. Using simulated neural spike signals, it has been shown that the RC system based on this device has the potential to directly process neural spikes. To increase the reservoir size of a single physical node, delayed feedback RC system, similar to the previous approach, has been successfully used for identifying neural discharge patterns, monitoring the transitions of discharge patterns, and identifying neural synchronization states among different neurons, as shown in Figs. 8(a–d). Advanced neuroelectronic systems with such memristor-based networks can achieve efficient analysis of neural signals with high spatiotemporal accuracy and may enable closed-loop feedback control, demonstrating the potential of using memristor-based RC systems for neural data analysis.

The electric-double-layer (EDL) formed at the interface between a semiconductor and an electrolyte can offer immense potential for constructing high-energy-efficient PRC. In the work of Yang [94], an EDL-coupled indium gallium zinc oxide (IGZO) artificial synapse was employed to achieve reservoir computing. The various reservoir states were obtained through a time-multiplexed masking process based on ion relaxation, where the ion-relaxation-coupled channel currents during different duration were accumulated N times using different masking matrices. This IGZO-based RC device exhibits nonlinearity, fading memory characteristics, and low average power consumption of 9.3 nW. Simulation-based recognition of handwritten [Figs. 8(e, f)] and spoken digit signals [Figs. 8(g, h)] resulted in energy consumption of 1.9 nJ per stored state and maximum accuracies of 90.86% and 100%, respectively. These results demonstrate the enormous potential of utilizing EDL coupling for achieving PRC.

3.3 Next generation reservoir computing

The underlying concept of RC is that the reservoir executes intricate nonlinear transformations on the input. By appropriately selecting the network and accurately sampling the readout, the intended output can be approximated. In contrast, methods like Nonlinear Vector Autoregression (NVAR) directly choose the nonlinear transformations of the input, which constitute the feature vector. The elements of this feature vector are then combined linearly to produce the output [95]. Notably, there exists a discernible similarity between RC and NVAR, and recent findings by Bollt have illustrated that these methods are equivalent under certain conditions [96]. Specifically, an RC employing linear activation nodes in conjunction with a feature vector that is a weighted sum of nonlinear functions of the reservoir node values is a comparably powerful universal approximator [97, 98]. Moreover, mathematically speaking, such an RC is equivalent to a nonlinear vector autoregression model. In the case of NVAR, the reservoir is no need, as the feature vector is composed to k time-delay observations of the dynamical system to be learned, as well as nonlinear functions of these observations [99].

Drawing inspiration from the research conducted by Bollt, Gauthier and his colleagues applied aspects of RC to NVAR, thereby introducing a novel approach termed next generation reservoir computing (NG-RC). Similar to what has been previously mentioned, NG-RC is a distinctive form of nonlinear vector autoregressive process that can be equivalently represented as a fusion of a reservoir with linear activation nodes and a nonlinear readout layer. The NG-RC model can be described as [100]

$$\begin{aligned}
&\boldsymbol{O}_{\mathrm{lin},i} = [\boldsymbol{X}(i), \boldsymbol{X}(i-s), \cdots, \boldsymbol{X}(i-(k-1)s)]^{\mathrm{T}},\\
&\boldsymbol{O}_{\mathrm{nonlin},i} = \boldsymbol{O}_{\mathrm{lin},i} \lceil\otimes\rceil \boldsymbol{O}_{\mathrm{lin},i},\\
&\boldsymbol{O}_{\mathrm{total},i} = c \otimes \boldsymbol{O}_{\mathrm{lin},i} \otimes \boldsymbol{O}_{\mathrm{nonlin},i},\\
&\boldsymbol{Y}(i) = \boldsymbol{W}_{\mathrm{out}} \boldsymbol{O}_{\mathrm{total},i}.
\end{aligned}$$

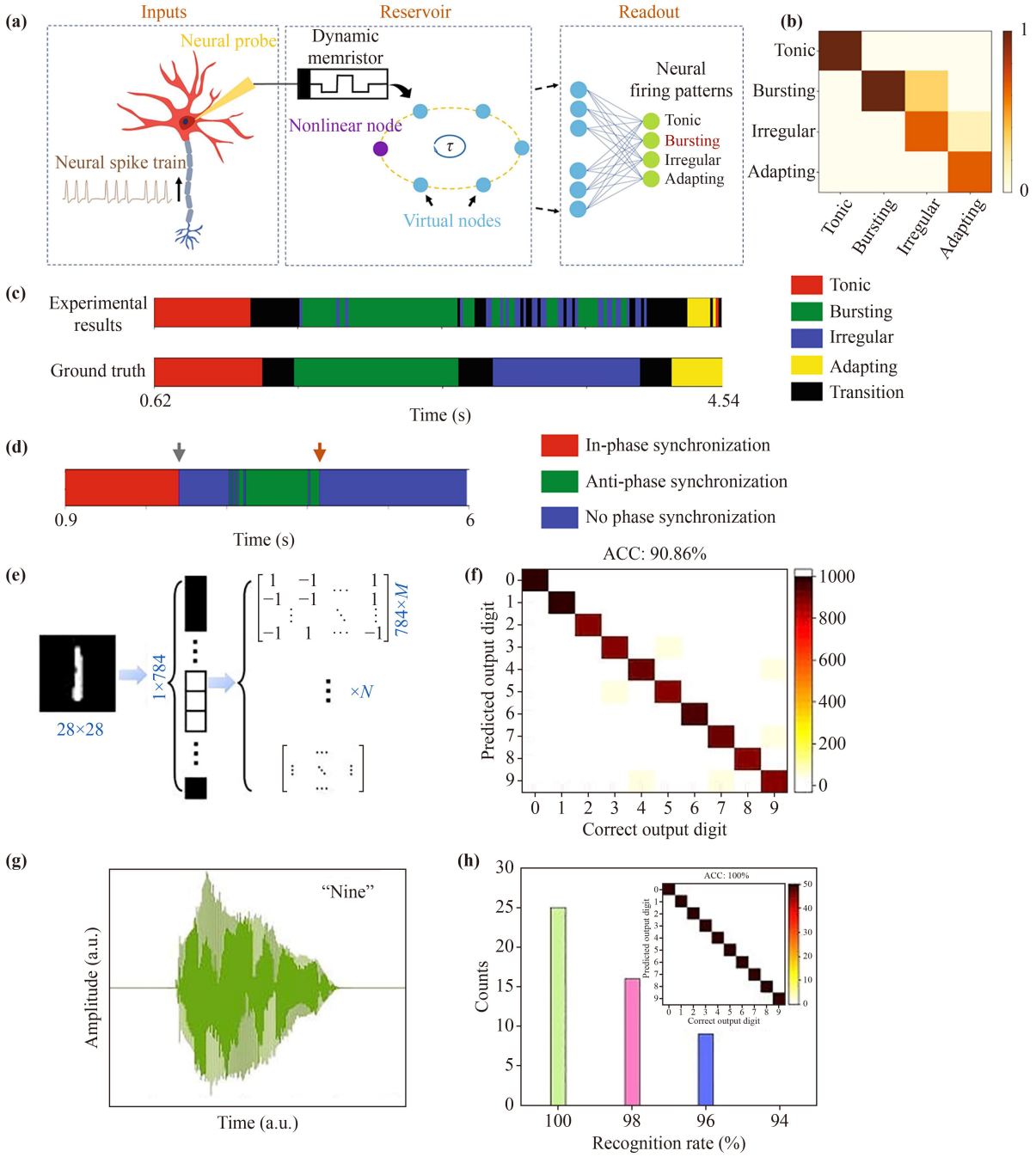

Fig. 8 **(a)** The delayed feedback RC system with virtual nodes for neural activity analysis. **(b)** False color confusion map. **(c)** Experimental results vs. ground truth in real-time analysis of neural firing pattern evolution. **(d)** Classification results in real-time analysis of neural synchronization. (a–d) Reproduced from Ref. [93]. **(e)** Schematic illustration of handwritten digit recognition. **(f)** False color confusion map, which is the result of handwritten digit recognition task. **(g)** Audio waveform corresponding to the digit nine pronounced by a speaker. **(h)** Results of spoken-digit recognition tasks. (e–h) Reproduced from Ref. [94].

Wherein, i is the discrete time, $\boldsymbol{O}_{\text{lin},i}$ is the linear feature vector, $\boldsymbol{X}(i)$ is the input vector at time i, s is the time interval, k represents the number of groups comprising the linear feature vector, $\boldsymbol{O}_{\text{nonlin},i}$ is the nonlinear feature vector at time i, $\lceil\otimes\rceil$ denotes the operator that performs the outer product of symbols on both sides and collects the unique monomials resulting from the outer product, $\boldsymbol{O}_{\text{total},i}$ denotes the total feature vector at time i, c as constant correction, $\boldsymbol{Y}(i)$ as the output value, $\boldsymbol{W}_{\text{out}}$ signifies the weight matrix connecting the reservoir to the output. Specifically, they utilize Tikhonov regularization and take into account correlations in the feature vector in

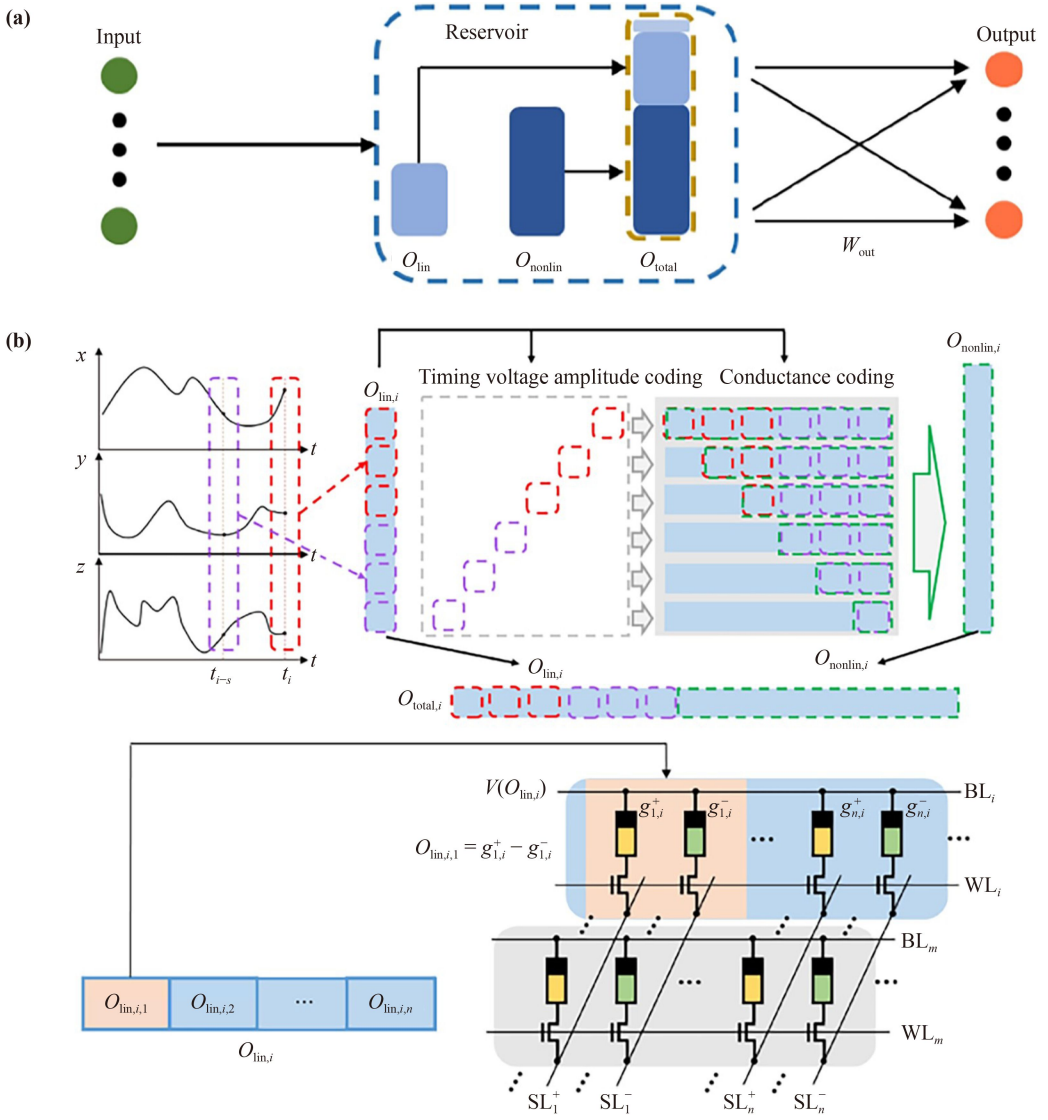

Fig. 9 **(a)** NG-RC, which is equivalent to nonlinear vector autoregression. **(b)** Structure of the NG-RC reservoir for three-dimensional timing signals predicting. (a, b) Reproduced from Ref. [100].

their approach. It yields favorable results in time-series prediction tasks, with several advantages over conventional RC. These advantages include fewer hyperparameters to tune due to the absence of a reservoir, a demonstrated requirement for shorter training data sets, and a smaller output vector dimension compared to the number of nodes in comparable reservoir computers. These factors also result in shorter computation times.

While the nonlinear transformation process in NG-RC circumvents the performance uncertainty and computational complexity associated with random connections in traditional reservoirs, it still requires substantial hardware and time overhead due to vector outer product operations and removal of redundant components from high-dimensional vectors. Ren *et al.* [100] proposed a hardware implementation method based on in-memory computing paradigm to simplify the NG-RC process, which involved matrix-vector multiplication (MVM) to represent the outer product between vectors and removing duplicate mapped vectors by preserving the values of fixed position elements after the outer product. In terms of hardware, memristor arrays were used for MVM operations, and selection line circuits of memristor arrays were used for preserving elements. The NG-RC process was simplified through matrix-vector multiplication operations, and system power consumption was reduced by utilizing memristor arrays for matrix-vector multiplication with time-varying voltage as input and conductance mapped to memristor arrays as weights, as shown in Fig. 9. The feasibility of this approach was verified through simulation experiments using the classic chaotic dynamical system model Lorenz63 for 3D time series prediction tasks. The simulation results showed that the prediction performance is closely related to the output accuracy and weight

accuracy. When the output accuracy reaches 16 bits, the further improvement of output accuracy has negligible impact on the prediction performance, and the system exhibited good noise robustness. When the weight accuracy reaches 8 bits, the short-term prediction (1 Lyapunov time) of Lorenz63 3D time series can achieve good prediction performance (NRMS less than 0.05), and it is also capable of long-term prediction to some extent.

The introduction of single-node delayed RC has made hardware implementation of RC more convenient, addressing to some extent the challenges associated with storage and update of neuron states in traditional reservoirs due to their large neuron populations. However, since virtual nodes are obtained through time division, the connectivity topology of delayed reservoirs is fixed in chronological order. It is implied that this type of delayed reservoir still faces difficulties in parameter optimization. One notable characteristic of NG-RC, in comparison to traditional RC, is the absence of a reservoir layer, resulting in fewer hyperparameters to be tuned and effectively addressing the issue of parameter optimization. Moreover, it is noteworthy that the use of memristor arrays in NG-RC for implementing the extensive multiplication operations offers faster computation speed and lower power consumption compared to traditional CMOS circuits.

4 Summary and outlook

As the fourth passive electronic component, memristor can store charges in a constantly changing electric field and retain them even after the field is removed, showing a high degree of similarity to synapses in the human brain. Therefore, memristors can be used to implement neuron models in brain science and for developing RC systems. Memristor-based RC has great development potential, as it can provide higher computing efficiency and lower energy consumption than traditional machine learning techniques. Memristor possess characteristics such as low power consumption, high density, rapid response, and programmability. With further research, the performance and stability of memristors have gradually improved, and manufacturing processes have also been enhanced, enabling the RC based on memristors to advance further. This technology can be widely applied in various fields, such as embedded systems, edge computing, large-scale data analysis, neuromorphic computing, and sensing applications.

In the field of embedded systems, the RC system can be applied in intelligent embedded devices, such as smart homes and smart watches. These devices typically have limited resources, and the efficiency and miniaturized design of RC system make it an algorithm very suitable for use in such devices. For example, it can be used in scenarios such as voice and gesture recognition in smart homes to increase the level of intelligence in embedded devices. In edge computing, RC can be used for intelligent processing in edge devices, thereby reducing data transmission costs. By running RC algorithms on edge devices, real-time analysis and response to sensor data on edge devices can be achieved, reducing network transmission volume and improving the efficiency and reliability of edge computing systems. In the field of large-scale data analysis, RC can be used for nonlinear data modeling and prediction. Compared with traditional machine learning algorithms, RC can better handle high-dimensional and time-series data, thereby improving the accuracy and reliability of data modeling. Additionally, the efficiency of RC also makes it an ideal algorithm for large-scale data analysis.

In the field of neuromorphic computing, memristor-based RC systems demonstrate several key benefits. Firstly, their high density allows for the integration of a large number of neurons and synapses in a compact space, facilitating the creation of large-scale neural networks. This high density is crucial for achieving complex and powerful computational capabilities. Additionally, memristors exhibit non-volatile memory properties, enabling the retention of information even when power is turned off. This characteristic results in energy-efficient computing as it reduces the need for continuous power supply and minimizes data transfer requirements. Memristor-based RC systems also excel in fast and parallel processing. They enable computations to be performed directly in memory, bypassing the need for data transfer between memory and processing units. This parallel processing capability accelerates computation speed, reduces latency, and makes the systems highly suitable for real-time applications where rapid decision-making is critical.

In the realm of sensing applications, memristor-based RC systems offer several advantages as well. Their high-density architecture enables efficient processing of large volumes of sensory data, leading to accurate and reliable pattern recognition. Sensor fusion is another area where memristor-based RC systems shine. By integrating data from multiple sensors and leveraging the parallel processing capabilities of the systems, sensor fusion can be achieved. Furthermore, memristor-based RC systems enable real-time processing of sensor data, making them ideal for time-critical applications. Whether it's environmental monitoring, industrial automation, or autonomous systems, the ability to process data in real-time allows for quick and accurate decision-making. Lastly, the high density of memristor-based RC systems enables the development of compact and portable sensing devices. These devices can seamlessly integrate into wearable technologies, Internet of Things (IoT) devices, and smart environments, facilitating the deployment of intelligent and efficient sensing capabilities.

In conclusion, the high density, low power consump-

tion, fast parallel processing, and sensor fusion capabilities of memristor-based RC systems make them invaluable for their potential application in future efficient and intelligent processing of large-scale data in various domains.

However, memristor-based RC also faces some challenges. Firstly, in large-scale reservoir computing, device-to-device variations of the memristor are inevitable, such as resistance range, switching behavior, and noise characteristics. These variations can introduce non-idealities to the RC system. They may arise due to manufacturing defects, material inhomogeneities, and environmental factors, leading to disparate responses among individual memristive devices and impacting the overall performance of the reservoir. In certain cases, the effects of device variations can be mitigated by employing appropriate training algorithms or compensation mechanisms. However, significant variations can result in unwanted distortions, increase the complexity of training, and reduce the overall accuracy and stability of the RC system. Furthermore, the manufacturing and integration technology of memristors is not yet fully mature, which limits their applied scope and reliability. In summary, memristors-based RC is still in its infancy and requires further research and development of algorithm, to meet the needs of various application scenarios.

Declarations The authors declare that they have no competing interests and there are no conflicts.

Acknowledgements This work was financially supported by the National Natural Science Foundation of China (Grant Nos. 11574057 and 12172093) and the Guangdong Basic and Applied Basic Research Foundation (Grant No. 2021A1515012607).

References and notes

1. J. Misra and I. Saha, Artificial neural networks in hardware: A survey of two decades of progress, *Neurocomputing* 74(1–3), 239 (2010)
2. Z. Liu, J. Tang, B. Gao, X. Li, P. Yao, Y. Lin, D. Liu, B. Hong, H. Qian, and H. Wu, Multichannel parallel processing of neural signals in memristor arrays, *Sci. Adv.* 6(41), eabc4797 (2020)
3. W. Wang and G. Zhou, Moisture influence in emerging neuromorphic device, *Front. Phys.* 18(5), 53601 (2023)
4. S. Ke, L. Jiang, Y. Zhao, Y. Xiao, B. Jiang, G. Cheng, F. Wu, G. Cao, Z. Peng, M. Zhu, and C. Ye, Brain-like synaptic memristor based on lithium-doped silicate for neuromorphic computing, *Front. Phys.* 17(5), 53508 (2022)
5. J. J. Hopfield, Neural networks and physical systems with emergent collective computational abilities, *Proc. Natl. Acad. Sci. USA* 79(8), 2554 (1982)
6. P. J. Werbos, Backpropagation through time: What it does and how to do it, *Proc. IEEE* 78(10), 1550 (1990)
7. M. Lukoševičius and H. Jaeger, Reservoir computing approaches to recurrent neural network training, *Comput. Sci. Rev.* 3(3), 127 (2009)
8. H. Jaeger, The "echo state" approach to analysing and training recurrent neural networks – with an Erratum note
9. P. Antonik, F. Duport, M. Hermans, A. Smerieri, M. Haelterman, and S. Massar, Online training of an opto-electronic reservoir computer applied to real-time channel equalization, *IEEE Trans. Neural Netw. Learn. Syst.* 28(11), 2686 (2017)
10. J. Lao, M. Yan, B. Tian, C. Jiang, C. Luo, Z. Xie, Q. Zhu, Z. Bao, N. Zhong, X. Tang, L. Sun, G. Wu, J. Wang, H. Peng, J. Chu, and C. Duan, Ultralow-power machine vision with self-powered sensor reservoir, *Adv. Sci. (Weinh.)* 9(15), 2106092 (2022)
11. M. Zhang, Z. Liang, and Z. R. Huang, Hardware optimization for photonic time-delay reservoir computer dynamics, *Neuromorph. Comput. Eng.* 3(1), 014008 (2023)
12. R. Nakane, G. Tanaka, and A. Hirose, Reservoir computing with spin waves excited in a garnet film, *IEEE Access* 6, 4462 (2018)
13. A. Papp, G. Csaba, and W. Porod, Characterization of nonlinear spin-wave interference by reservoir-computing metrics, *Appl. Phys. Lett.* 119(11), 112403 (2021)
14. J. Moon, W. Ma, J. H. Shin, F. Cai, C. Du, S. H. Lee, and W. D. Lu, Temporal data classification and forecasting using a memristor-based reservoir computing system, *Nat. Electron.* 2(10), 480 (2019)
15. H. Coy, R. Cabrera, N. Sepúlveda, and F. E. Fernández, Optoelectronic and all-optical multiple memory states in vanadium dioxide, *J. Appl. Phys.* 108(11), 113115 (2010)
16. K. Liu, C. Cheng, J. Suh, R. Tang-Kong, D. Fu, S. Lee, J. Zhou, L. O. Chua, and J. Wu, Powerful, multifunctional torsional micromuscles activated by phase transition, *Adv. Mater.* 26(11), 1746 (2014)
17. W. Yi, K. K. Tsang, S. K. Lam, X. Bai, J. A. Crowell, and E. A. Flores, Biological plausibility and stochasticity in scalable VO_2 active memristor neurons, *Nat. Commun.* 9(1), 4661 (2018)
18. M. Ismail, H. Abbas, C. Choi, and S. Kim, Controllable analog resistive switching and synaptic characteristics in ZrO_2/ZTO bilayer memristive device for neuromorphic systems, *Appl. Surf. Sci.* 529, 147107 (2020)
19. M. Ismail, H. Abbas, C. Choi, and S. Kim, Stabilized and RESET-voltage controlled multi-level switching characteristics in ZrO_2-based memristors by inserting a-ZTO interface layer, *J. Alloys Compd.* 835, 155256 (2020)
20. S. G. Hu, Y. Liu, T. P. Chen, Z. Liu, Q. Yu, L. J. Deng, Y. Yin, and S. Hosaka, Emulating the Ebbinghaus forgetting curve of the human brain with a NiO-based memristor, *Appl. Phys. Lett.* 103(13), 133701 (2013)
21. Y. Li, J. Chu, W. Duan, G. Cai, X. Fan, X. Wang, G. Wang, and Y. Pei, Analog and digital bipolar resistive switching in solution-combustion-processed NiO memristor, *ACS Appl. Mater. Interfaces* 10(29), 24598 (2018)
22. V. Q. Le, T. H. Do, J. R. D. Retamal, P. W. Shao, Y. H. Lai, W. W. Wu, J. H. He, Y. L. Chueh, and Y. H.

Chu, Van der Waals heteroepitaxial AZO/NiO/AZO/muscovite (ANA/muscovite) transparent flexible memristor, *Nano Energy* 56, 322 (2019)
23. L. Zhang, Z. Tang, J. Fang, X. Jiang, Y. P. Jiang, Q. J. Sun, J. M. Fan, X. G. Tang, and G. Zhong, Synaptic and resistive switching behaviors in NiO/Cu_2O heterojunction memristor for bioinspired neuromorphic computing, *Appl. Surf. Sci.* 606, 154718 (2022)
24. T. Chang, S. H. Jo, K. H. Kim, P. Sheridan, S. Gaba, and W. Lu, Synaptic behaviors and modeling of a metal oxide memristive device, *Appl. Phys. A* 102(4), 857 (2011)
25. J. Moon, W. Ma, J. H. Shin, F. Cai, C. Du, S. H. Lee, and W. D. Lu, Temporal data classification and forecasting using a memristor-based reservoir computing system, *Nat. Electron.* 2(10), 480 (2019)
26. J. Shin, M. Kang, and S. Kim, Gradual conductance modulation of Ti/WO_x/Pt memristor with self-rectification for a neuromorphic system, *Appl. Phys. Lett.* 119(1), 012102 (2021)
27. Y. Tao, Z. Wang, H. Xu, W. Ding, X. Zhao, Y. Lin, and Y. Liu, Moisture-powered memristor with interfacial oxygen migration for power-free reading of multiple memory states, *Nano Energy* 71, 104628 (2020)
28. L. Zhang, Z. Tang, D. Yao, Z. Fan, S. Hu, Q. J. Sun, X. G. Tang, Y. P. Jiang, X. Guo, M. Huang, G. Zhong, and J. Gao, Synaptic behaviors in flexible Au/WO_x/Pt/mica memristor for neuromorphic computing system, *Mater. Today Phys.* 23, 100650 (2022)
29. C. H. Huang, J. S. Huang, S. M. Lin, W. Y. Chang, J. H. He, and Y. L. Chueh, ZnO_{1-x} nanorod arrays/ZnO thin film bilayer structure: from homojunction diode and high-performance memristor to complementary 1D1R application, *ACS Nano* 6(9), 8407 (2012)
30. J. Park, S. Lee, J. Lee, and K. Yong, A light incident angle switchable ZnO nanorod memristor: Reversible switching behavior between two non-volatile memory devices, *Adv. Mater.* 25(44), 6423 (2013)
31. A. Kumar, M. Das, V. Garg, B. S. Sengar, M. T. Htay, S. Kumar, A. Kranti, and S. Mukherjee, Forming-free high-endurance Al/ZnO/Al memristor fabricated by dual ion beam sputtering, *Appl. Phys. Lett.* 110(25), 253509 (2017)
32. S. Dirkmann, J. Kaiser, C. Wenger, and T. Mussenbrock, Filament growth and resistive switching in hafnium oxide memristive devices, *ACS Appl. Mater. Interfaces* 10(17), 14857 (2018)
33. B. Ku, Y. Abbas, S. Kim, A. S. Sokolov, Y. R. Jeon, and C. Choi, Improved resistive switching and synaptic characteristics using Ar plasma irradiation on the Ti/HfO_2 interface, *J. Alloys Compd.* 797, 277 (2019)
34. G. S. Kim, H. Song, Y. K. Lee, J. H. Kim, W. Kim, T. H. Park, H. J. Kim, K. Min Kim, and C. S. Hwang, Defect-engineered electroforming-free analog HfO_x memristor and its application to the neural network, *ACS Appl. Mater. Interfaces* 11(50), 47063 (2019)
35. M. J. Lee, C. B. Lee, D. Lee, S. R. Lee, M. Chang, J. H. Hur, Y. B. Kim, C. J. Kim, D. H. Seo, S. Seo, U. I. Chung, I. K. Yoo, and K. Kim, A fast, high-endurance and scalable non-volatile memory device made from asymmetric Ta_2O_{5-x}/TaO_{2-x} bilayer structures, *Nat. Mater.* 10(8), 625 (2011)
36. J. Joshua Yang, M. X. Zhang, M. D. Pickett, F. Miao, J. Paul Strachan, W. D. Li, W. Yi, D. A. A. Ohlberg, B. Joon Choi, W. Wu, J. H. Nickel, G. Medeiros-Ribeiro, and R. S. Williams, Engineering nonlinearity into memristors for passive crossbar applications, *Appl. Phys. Lett.* 100(11), 113501 (2012)
37. F. Miao, W. Yi, I. Goldfarb, J. J. Yang, M. X. Zhang, M. D. Pickett, J. P. Strachan, G. Medeiros-Ribeiro, and R. S. Williams, Continuous electrical tuning of the chemical composition of TaO_x-based memristors, *ACS Nano* 6(3), 2312 (2012)
38. Z. Wang, M. Yin, T. Zhang, Y. Cai, Y. Wang, Y. Yang, and R. Huang, Engineering incremental resistive switching in TaO_x based memristors for brain-inspired computing, *Nanoscale* 8(29), 14015 (2016)
39. L. H. Li, K. H. Xue, L. Q. Zou, J. H. Yuan, H. Sun, and X. Miao, Multilevel switching in Mg-doped HfO_x memristor through the mutual-ion effect, *Appl. Phys. Lett.* 119(15), 153505 (2021)
40. J. H. Ryu, C. Mahata, and S. Kim, Long-term and short-term plasticity of Ta_2O_5/HfO_2 memristor for hardware neuromorphic application, *J. Alloys Compd.* 850, 156675 (2021)
41. A. Saleem, F. M. Simanjuntak, S. Chandrasekaran, S. Rajasekaran, T. Y. Tseng, and T. Prodromakis, Transformation of digital to analog switching in TaO_x-based memristor device for neuromorphic applications, *Appl. Phys. Lett.* 118(11), 112103 (2021)
42. L. Du, Z. Wang, and G. Zhao, Novel intelligent devices: Two-dimensional materials based memristors, *Front. Phys.* 17(2), 23602 (2022)
43. Z. Zhou, F. Yang, S. Wang, L. Wang, X. Wang, C. Wang, Y. Xie, and Q. Liu, Emerging of two-dimensional materials in novel memristor, *Front. Phys.* 17(2), 23204 (2022)
44. Y. T. Chan, Y. Fu, L. Yu, F. Y. Wu, H. W. Wang, T. H. Lin, S. H. Chan, M. C. Wu, and J. C. Wang, Compacted self-assembly graphene with hydrogen plasma surface modification for robust artificial electronic synapses of gadolinium oxide memristors, *Adv. Mater. Interfaces* 7(20), 2000860 (2020)
45. X. Zhao, J. Ma, X. Xiao, Q. Liu, L. Shao, D. Chen, S. Liu, J. Niu, X. Zhang, Y. Wang, R. Cao, W. Wang, Z. Di, H. Lv, S. Long, and M. Liu, Breaking the current-retention dilemma in cation-based resistive switching devices utilizing graphene with controlled defects, *Adv. Mater.* 30(14), 1705193 (2018)
46. J. Lee, C. Du, K. Sun, E. Kioupakis, and W. D. Lu, Tuning ionic transport in memristive devices by graphene with engineered nanopores, *ACS Nano* 10(3), 3571 (2016)
47. M. Naqi, et al., Multilevel artificial electronic synaptic device of direct grown robust MoS_2 based memristor array for in-memory deep neural network, *npj 2D Mater. Appl.* 6, 53 (2022)
48. X. Yan, Q. Zhao, A. P. Chen, J. Zhao, Z. Zhou, J. Wang, H. Wang, L. Zhang, X. Li, Z. Xiao, K. Wang, C. Qin, G. Wang, Y. Pei, H. Li, D. Ren, J. Chen, and Q. Liu, Vacancy-induced synaptic behavior in 2D WS_2 nanosheet-based memristor for low-power neuromorphic

computing, *Small* 15(24), 1901423 (2019)
49. Z. Xie, Y. Duo, Z. Lin, T. Fan, C. Xing, L. Yu, R. Wang, M. Qiu, Y. Zhang, Y. Zhao, X. Yan, and H. Zhang, The rise of 2D photothermal materials beyond graphene for clean water production, *Adv. Sci. (Weinh.)* 7(5), 1902236 (2020)
50. S. Manzeli, D. Ovchinnikov, D. Pasquier, O. V. Yazyev, and A. Kis, 2D transition metal dichalcogenides, *Nat. Rev. Mater.* 2(8), 17033 (2017)
51. Y. Shi, X. Liang, B. Yuan, V. Chen, H. Li, F. Hui, Z. Yu, F. Yuan, E. Pop, H. S. P. Wong, and M. Lanza, Electronic synapses made of layered two-dimensional materials, *Nat. Electron.* 1(8), 458 (2018)
52. C. Moreno, C. Munuera, S. Valencia, F. Kronast, X. Obradors, and C. Ocal, Reversible resistive switching and multilevel recording in $La_{0.7}Sr_{0.3}MnO_3$ thin films for low cost nonvolatile memories, *Nano Lett.* 10(10), 3828 (2010)
53. D. Liu, N. Wang, G. Wang, Z. Shao, X. Zhu, C. Zhang, and H. Cheng, Nonvolatile bipolar resistive switching in amorphous Sr-doped $LaMnO_3$ thin films deposited by radio frequency magnetron sputtering, *Appl. Phys. Lett.* 102(13), 134105 (2013)
54. D. Liu, H. Cheng, X. Zhu, G. Wang, and N. Wang, Analog memristors based on thickening/thinning of Ag nanofilaments in amorphous manganite thin films, *ACS Appl. Mater. Interfaces* 5(21), 11258 (2013)
55. N. Lee, Y. Lansac, H. Hwang, and Y. H. Jang, Switching mechanism of $Al/La_{1-x}Sr_xMnO_3$ resistance random access memory. I. Oxygen vacancy formation in perovskites, *RSC Adv.* 5(124), 102772 (2015)
56. K. Szot, W. Speier, G. Bihlmayer, and R. Waser, Switching the electrical resistance of individual dislocations in single-crystalline $SrTiO_3$, *Nat. Mater.* 5(4), 312 (2006)
57. Z. Hu, Q. Li, M. Li, Q. Wang, Y. Zhu, X. Liu, X. Zhao, Y. Liu, and S. Dong, Ferroelectric memristor based on $Pt/BiFeO_3/Nb$-doped $SrTiO_3$ heterostructure, *Appl. Phys. Lett.* 102(10), 102901 (2013)
58. F. Messerschmitt, M. Kubicek, S. Schweiger, and J. L. M. Rupp, Memristor kinetics and diffusion characteristics for mixed anionic-electronic $SrTiO_{3-\delta}$ bits: The memristor-based cottrell analysis connecting material to device performance, *Adv. Funct. Mater.* 24(47), 7448 (2014)
59. Z. H. Shen, W. H. Li, X. G. Tang, J. Hu, K. Y. Wang, Y. P. Jiang, and X. B. Guo, An artificial synapse based on Sr(Ti, Co)O_3 films, *Mater. Today Commun.* 33, 104754 (2022)
60. X. Yan, X. Han, Z. Fang, Z. Zhao, Z. Zhang, J. Sun, Y. Shao, Y. Zhang, L. Wang, S. Sun, Z. Guo, X. Jia, Y. Zhang, Z. Guan, and T. Shi, Reconfigurable memristor based on $SrTiO_3$ thin-film for neuromorphic computing, *Front. Phys.* 18(6), 63301 (2023)
61. J. Q. Yang, R. Wang, Z. P. Wang, Q. Y. Ma, J. Y. Mao, Y. Ren, X. Yang, Y. Zhou, and S. T. Han, Leaky integrate-and-fire neurons based on perovskite memristor for spiking neural networks, *Nano Energy* 74, 104828 (2020)
62. L. Wang, J. Sun, Y. Zhang, J. Niu, Z. Zhao, Z. Guo, Z. Zhang, Y. Shao, S. Sun, X. Jia, X. Han, and X. Yan, Ferroelectric memristor based on Li-doped $BiFeO_3$ for information processing, *Appl. Phys. Lett.* 121(24), 241901 (2022)
63. F. Luo, W. M. Zhong, X. G. Tang, J. Y. Chen, Y. P. Jiang, and Q. X. Liu, Application of artificial synapse based on all-inorganic perovskite memristor in neuromorphic computing, *Nano Mater. Sci.*, S258996512300003X (2023)
64. W. M. Zhong, X. G. Tang, L. L. Bai, J. Y. Chen, H. F. Dong, Q. J. Sun, Y. P. Jiang, and Q. X. Liu, A halide perovskite thin film diode with modulated depletion layers for artificial synapse, *J. Alloys Compd.* 960, 170773 (2023)
65. F. Ye, X. G. Tang, J. Y. Chen, W. M. Zhong, L. Zhang, Y. P. Jiang, and Q. X. Liu, Neurosynaptic-like behavior of Ce-doped $BaTiO_3$ ferroelectric thin film diodes for visual recognition applications, *Appl. Phys. Lett.* 121(17), 171901 (2022)
66. W. M. Zhong, X. G. Tang, Q. X. Liu, and Y. P. Jiang, Artificial optoelectronic synaptic characteristics of Bi_2FeMnO_6 ferroelectric memristor for neuromorphic computing, *Mater. Des.* 222, 111046 (2022)
67. R. Su, R. Xiao, C. Shen, D. Song, J. Chen, B. Zhou, W. Cheng, Y. Li, X. Wang, and X. Miao, Oxygen ion migration induced polarity switchable $SrFeO_x$ memristor for high-precision handwriting recognition, *Appl. Surf. Sci.* 617, 156620 (2023)
68. D. A. Lapkin, A. V. Emelyanov, V. A. Demin, V. V. Erokhin, L. A. Feigin, P. K. Kashkarov, and M. V. Kovalchuk, Polyaniline-based memristive microdevice with high switching rate and endurance, *Appl. Phys. Lett.* 112(4), 043302 (2018)
69. D. A. Lapkin, A. V. Emelyanov, V. A. Demin, T. S. Berzina, and V. V. Erokhin, Spike-timing-dependent plasticity of polyaniline-based memristive element, *Microelectron. Eng.* 185–186, 43 (2018)
70. Y. Gerasimov, E. Zykov, N. Prudnikov, M. Talanov, A. Toschev, and V. Erokhin, On the organic memristive device resistive switching efficacy, *Chaos Solitons Fractals* 143, 110549 (2021)
71. S. Li, F. Zeng, C. Chen, H. Liu, G. Tang, S. Gao, C. Song, Y. Lin, F. Pan, and D. Guo, Synaptic plasticity and learning behaviours mimicked through Ag interface movement in an Ag/conducting polymer/Ta memristive system, *J. Mater. Chem. C* 1(34), 5292 (2013)
72. S. Ali, J. Bae, K. H. Choi, C. H. Lee, Y. H. Doh, S. Shin, and N. P. Kobayashi, Organic non-volatile memory cell based on resistive elements through electro-hydrodynamic technique, *Org. Electron.* 17, 121 (2015)
73. V. C. Nguyen and P. S. Lee, Coexistence of write once read many memory and memristor in blend of Poly(3, 4-ethylenedioxythiophene): Polystyrene sulfonate and polyvinyl alcohol, *Sci. Rep.* 6(1), 38816 (2016)
74. L. P. Ma, J. Liu, and Y. Yang, Organic electrical bistable devices and rewritable memory cells, *Appl. Phys. Lett.* 80(16), 2997 (2002)
75. M. Kano, S. Orito, Y. Tsuruoka, and N. Ueno, Nonvolatile memory effect of an Al/2-Amino-4, 5-dicyanoimidazole/Al structure, *Synth. Met.* 153(1–3), 265 (2005)

76. M. Terai, K. Fujita, and T. Tsutsui, Electrical bistability of organic thin-film device using Ag electrode, *Jpn. J. Appl. Phys.* 45(4B), 3754 (2006)
77. Y. Zhao, W. J. Sun, J. Wang, J. H. He, H. Li, Q. F. Xu, N. J. Li, D. Y. Chen, and J. M. Lu, All-inorganic ionic polymer-based memristor for high-performance and flexible artificial synapse, *Adv. Funct. Mater.* 30(39), 2004245 (2020)
78. J. Li, Y. Qian, W. Li, Y. H. Lin, H. Qian, T. Zhang, K. Sun, J. Wang, J. Zhou, Y. Chen, J. Zhu, G. Zhang, M. Yi, and W. Huang, Humidity-enabled organic artificial synaptic devices with ultrahigh moisture resistivity, *Adv. Electron. Mater.* 8(10), 2200320 (2022)
79. Y. Park and J. S. Lee, Artificial synapses with short- and long-term memory for spiking neural networks based on renewable materials, *ACS Nano* 11(9), 8962 (2017)
80. W. M. Zhong, C. L. Luo, X. G. Tang, X. B. Lu, and J. Y. Dai, Dynamic FET-based memristor with relaxor antiferroelectric HfO_2 gate dielectric for fast reservoir computing, *Mater. Today Nano* 23, 100357 (2023)
81. E. Choi, A. Schuetz, W. F. Stewart, and J. Sun, Using recurrent neural network models for early detection of heart failure onset, *J. Am. Med. Inform. Assoc.* 24(2), 361 (2017)
82. W. Maass, T. Natschläger, and H. Markram, Real-time computing without stable states: A new framework for neural computation based on perturbations, *Neural Comput.* 14(11), 2531 (2002)
83. G. Zhang, Z. Y. Xiong, Y. Gong, Z. Zhu, Z. Lv, Y. Wang, J. Q. Yang, X. Xing, Z. P. Wang, J. Qin, Y. Zhou, and S. T. Han, Polyoxometalate accelerated cationic migration for reservoir computing, *Adv. Funct. Mater.* 32(45), 2204721 (2022)
84. C. Du, F. Cai, M. A. Zidan, W. Ma, S. H. Lee, and W. D. Lu, Reservoir computing using dynamic memristors for temporal information processing, *Nat. Commun.* 8(1), 2204 (2017)
85. G. Milano, G. Pedretti, K. Montano, S. Ricci, S. Hashemkhani, L. Boarino, D. Ielmini, and C. Ricciardi, In materia reservoir computing with a fully memristive architecture based on self-organizing nanowire networks, *Nat. Mater.* 21(2), 195 (2022)
86. A. N. Matsukatova, N. V. Prudnikov, V. A. Kulagin, S. Battistoni, A. A. Minnekhanov, A. D. Trofimov, A. A. Nesmelov, S. A. Zavyalov, Y. N. Malakhova, M. Parmeggiani, A. Ballesio, S. L. Marasso, S. N. Chvalun, V. A. Demin, A. V. Emelyanov, and V. Erokhin, Combination of organic-based reservoir computing and spiking neuromorphic systems for a robust and efficient pattern classification, *Adv. Intell. Syst.* 5(6), 2200407 (2023)
87. N. V. Prudnikov, V. A. Kulagin, S. Battistoni, V. A. Demin, V. V. Erokhin, and A. V. Emelyanov, Polyaniline -based memristive devices as key elements of robust reservoir computing for image classification, *Phys. Status Solidi A* 220(11), 2200700 (2023)
88. A. A. Koroleva, D. S. Kuzmichev, M. G. Kozodaev, I. V. Zabrosaev, E. V. Korostylev, and A. M. Markeev, CMOS-compatible self-aligned 3D memristive elements for reservoir computing systems, *Appl. Phys. Lett.* 122(2), 022905 (2023)
89. L. Appeltant, M. C. Soriano, G. Van der Sande, J. Danckaert, S. Massar, J. Dambre, B. Schrauwen, C. R. Mirasso, and I. Fischer, Information processing using a single dynamical node as complex system, *Nat. Commun.* 2(1), 468 (2011)
90. L. Appeltant, G. Van der Sande, J. Danckaert, and I. Fischer, Constructing optimized binary masks for reservoir computing with delay systems, *Sci. Rep.* 4(1), 3629 (2014)
91. Y. Zhong, J. Tang, X. Li, B. Gao, H. Qian, and H. Wu, Dynamic memristor-based reservoir computing for high-efficiency temporal signal processing, *Nat. Commun.* 12(1), 408 (2021)
92. Y. Zhong, J. Tang, X. Li, X. Liang, Z. Liu, Y. Li, Y. Xi, P. Yao, Z. Hao, B. Gao, H. Qian, and H. Wu, A memristor-based analogue reservoir computing system for real-time and power-efficient signal processing, *Nat. Electron.* 5(10), 672 (2022)
93. X. Zhu, Q. Wang, and W. D. Lu, Memristor networks for real-time neural activity analysis, *Nat. Commun.* 11(1), 2439 (2020)
94. Y. Yang, H. Cui, S. Ke, M. Pei, K. Shi, C. Wan, and Q. Wan, Reservoir computing based on electric-double-layer coupled InGaZnO artificial synapse, *Appl. Phys. Lett.* 122(4), 043508 (2023)
95. L. Jaurigue and K. Lüdge, Connecting reservoir computing with statistical forecasting and deep neural networks, *Nat. Commun.* 13(1), 227 (2022)
96. E. Bollt, On explaining the surprising success of reservoir computing forecaster of chaos? The universal machine learning dynamical system with contrast to VAR and DMD, *Chaos* 31(1), 013108 (2021)
97. L. Gonon and J. P. Ortega, Reservoir computing universality with stochastic inputs, *IEEE Trans. Neural Netw. Learn. Syst.* 31(1), 100 (2020)
98. A. G. Hart, J. L. Hook, and J. H. P. Dawes, Echo State Networks trained by Tikhonov least squares are $L^2(\mu)$ approximators of ergodic dynamical systems, *Physica D* 421, 132882 (2021)
99. D. J. Gauthier, E. Bollt, A. Griffith, and W. A. S. Barbosa, Next generation reservoir computing, *Nat. Commun.* 12(1), 5564 (2021)
100. K. Ren, W. Y. Zhang, F. Wang, Z. Y. Guo, and D. S. Shang, Next-generation reservoir computing based on memristor array, *Acta Physica Sinica* 71(14), 140701 (2022)